Universiteit
Leiden
The Netherlands

Computational modeling of pharmacokinetics and tumor dynamics to guide anti-cancer treatment

Yin, A.

Citation
Yin, A. (2024, February 1). *Computational modeling of pharmacokinetics and tumor dynamics to guide anti-cancer treatment*. Retrieved from https://hdl.handle.net/1887/3715801

Version:	Publisher's Version
License:	Licence agreement concerning inclusion of doctoral thesis in the Institutional Repository of the University of Leiden
Downloaded from:	https://hdl.handle.net/1887/3715801

Note: To cite this publication please use the final published version (if applicable).

Section I

Modeling tumor dynamics including treatment resistance

Chapter 2

A review of mathematical models for tumor dynamics and treatment resistance evolution of solid tumors

Anyue Yin, Dirk Jan A.R. Moes, Johan G.C. van Hasselt,
Jesse J. Swen, Henk-Jan Guchelaar

CPT Pharmacometrics Syst Pharmacol. 2019 Oct;8(10):720-737

Abstract

Increasing knowledge of intertumor heterogeneity, intratumor heterogeneity, and cancer evolution has improved the understanding of anticancer treatment resistance. A better characterization of cancer evolution and subsequent use of this knowledge for personalized treatment would increase the chance to overcome cancer treatment resistance. Model-based approaches may help achieve this goal. In this review, we comprehensively summarized mathematical models of tumor dynamics for solid tumors and of drug resistance evolution. Models displayed by ordinary differential equations, algebraic equations, and partial differential equations for characterizing tumor burden dynamics are introduced and discussed. As for tumor resistance evolution, stochastic and deterministic models are introduced and discussed. The results may facilitate a novel model-based analysis on anticancer treatment response and the occurrence of resistance, which incorporates both tumor dynamics and resistance evolution. The opportunities of a model-based approach as discussed in this review can be of great benefit for future optimizing and personalizing anticancer treatment.

1. Introduction

Drug resistance is one of the major reasons for patients experiencing treatment failure in the area of oncology [1]. Increasing knowledge of intertumor and intratumor heterogeneity that suggests distinct cells exist in different or the same tumors as well as cancer evolution have improved the understanding of anticancer treatment resistance [2]. It thereby pushes forward the necessity of precision medicine rather than a one-size-fits-all approach [2]. To rationalize the treatment personalization and address treatment failure, the use of modeling and simulation, which can quantitatively characterize and predict the relationships between drug exposure/pharmacokinetics (PK), drug effects/pharmacodynamics (PD), and disease progression, is widely accepted to support drug decision making [3-6].

Mathematical models that characterize the effects of anticancer drug treatment for solid tumors based on tumor size dynamics, which is typically quantified with measurements of tumor diameter and volume, represent one key class of models applied in cancer pharmacology. Various tumor growth modeling strategies have been previously reviewed, including agent-based models [7], image-based models [8], multiscale models [9], and PK/PD models [10, 11].

Currently, an increasing number of studies concerning the gene sequencing of tumor biopsies in different cancer types have demonstrated the dynamics of cancer evolution [2, 12]. Intratumor heterogeneity that results from cancer evolution and an evolving adaption of heterogeneous tumor to treatment are also increasingly acknowledged as key factors related to the development of resistance [2, 12]. To better characterize this process and to account for tumor heterogeneity, mathematical models that consider the evolution of tumors have been proposed [13-17]. Potentially, such evolution models in conjunction with tumor growth models could be of benefit to interpret both tumor size change and evolving tumor progression during treatment and thereby ultimately rationalize adaptive treatments for individual patients and overcome treatment resistance.

To identify the challenges and opportunities of characterizing tumor size change and resistance evolution simultaneously with a model-based approach that can facilitate anticancer treatment optimization and personalized medicine, an overview of the current available model structures is needed. Thus, in the current review, we comprehensively summarized mathematical models for the characterization of tumor growth (inhibition) dynamics in solid tumors and the relevant clonal evolution of drug resistance by a systematic search and study of previous literature. The focus in this review lies particularly on models that are applicable for clinical data.

2. Literature search

Studies that characterized tumor growth (inhibition) dynamics and clonal evolution of drug resistance with mathematical models were systematically retrieved and studied from the PubMed database to provide a comprehensive and unbiased review. In total, 274 and 85 publications were obtained, respectively, for studies of tumor dynamics and tumor resistance evolution based on established search terms. Details of the literature search are described in **Supplementary Material S2.1** and **Figure S2.1**. Ultimately, 61 and 25 papers, among which 13 and 2 papers were obtained from the publications' references, which introduced corresponding original models or demonstrated application examples of certain model structures, were included, respectively, for tumor dynamics and resistance evolution modeling. Model structures, cancer types, treatments, and the ways of reporting tumor sizes were extracted from the included papers. The identified model structures were classified by equation types in later sessions and were summarized in **Tables 2.1** and **2.2**. Data input, knowledge requirement, study type, and objectives related to different model structures were summarized in **Table 2.3** to provide a reference of the selection of different model structures. The information of software that was used to perform the corresponding modeling and simulation analysis was also obtained and are summarized in **Supplementary Material S2.1** and **Table S2.1**.

3. Tumor dynamics modeling

3.1 Ordinary differential equation

3.1.1 Basic growth model

A majority of the included studies applied ordinary differential equations (ODEs) to describe tumor burden change. The natural growth of a tumor without treatment is commonly characterized with several basic functions, including linear, exponential, logistic, Gompertz, and combined exponential and linear models (**Table 2.1**). The time curves of different models were simulated and are presented in **Figure 2.1**. Differential equations were solved with the RxODE package implemented in R software (version 3.4.1; R Foundation for Statistical Computing, Vienna, Austria).

The linear tumor growth assumes a constant zero-order growth rate (Eq. 2.1; **Figure 2.1**) [10]. It has been applied to describe the natural tumor growth of metastatic renal cell carcinoma [18] based on the measurements of sum of longest diameters (SLD) of the target lesions in patients.

Table 2.1: Modeling frameworks for characterizing tumor dynamics

Models/assumptions	Equations		Ref.
Ordinary differential equations			
Basic functions describing natural tumor growth			
Linear growth	$\frac{dT}{dt} = k_g$	Eq. 2.1	[18]
	$\frac{dT}{dt} = k_g - d \cdot T$	Eq. 2.2	[21]
Exponential growth	$\frac{dT}{dt} = k_g \cdot T$	Eq. 2.3	[20]
	$\frac{dT}{dt} = k_g \cdot T - d \cdot T$	Eq. 2.4	[22, 23]
Logistic growth	$\frac{dT}{dt} = k_g \cdot T \cdot \left(1 - \frac{T}{T_{max}}\right)$	Eq. 2.5	[24, 25]
Gompertz growth	$\frac{dT}{dt} = k_g \cdot T \cdot \ln\left(\frac{T_{max}}{T}\right)$	Eq. 2.6	[27, 29]
	$\frac{dlnT}{dt} = a - blnT$	Eq. 2.7	[28]
Combination of exponential and linear growth	$\frac{dT}{dt} = \frac{\lambda_0 \cdot T}{\left[1 + \left(\frac{\lambda_0}{\lambda_1} \cdot T\right)^{20}\right]^{\frac{1}{20}}}$	Eq. 2.8	[31]
Model structures integrating tumor heterogeneity			
Tumor burden(T)= Proliferative component (P) + Quiescent component (Q)	$\begin{cases} \frac{dP}{dt} = f(P) - m_1 \cdot P \\ \frac{dQ}{dt} = m_1 \cdot P \end{cases}$	Eq. 2.9	[25]
	$\begin{cases} \frac{dP}{dt} = f(P) - m_1 \cdot P + m_2 \cdot Q \\ \frac{dQ}{dt} = m_1 \cdot P - m_2 \cdot Q \end{cases}$	Eq. 2.10	[22, 33]
Tumor burden (T)= Sensitive component (S) + Resistant component (R)	$\begin{cases} \frac{dS}{dt} = f(S) \\ \frac{dR}{dt} = f(R) \end{cases}$	Eq. 2.11	[24]

Table 2.1 continues on next page.

Table 2.1: *Continued*

Models/assumptions	Equations		Ref.
Tumor burden (T)= Sensitive component (S) + Resistant component (R)	$\begin{cases} \frac{dS}{dt} = f(S) - m_1 \cdot S \\ \frac{dR}{dt} = f(R) + m_1 \cdot S \end{cases}$	Eq. 2.12	[23, 35]
	$\begin{cases} \frac{dS}{dt} = f(S) - m_1 \cdot S + m_2 \cdot R \\ \frac{dR}{dt} = f(R) + m_1 \cdot S - m_2 \cdot R \end{cases}$	Eq. 2.13	[34, 36]
Model structures integrating tumor biology process			
Angiogenesis	$\frac{dT}{dt} = f(T) - k \cdot \frac{BM_0 - BM_t}{BM_0} \cdot T$ $= f(T) - k \cdot \left(1 - \frac{BM_t}{BM_0}\right) \cdot T$	Eq. 2.14	[31, 39]
	$\begin{cases} \frac{dT}{dt} = k_g \cdot T \cdot \left(1 - \frac{T}{E}\right) \\ \frac{dE}{dt} = k_2 \cdot T^{\frac{1}{2}} \end{cases}$	Eq. 2.15	[40]
	$\begin{cases} \frac{dT}{dt} = k_g \cdot V \cdot \log\left(\frac{E}{T}\right) \\ \frac{dE}{dt} = k_2 \cdot T - d \cdot T^{\frac{2}{3}} \cdot E \end{cases}$	Eq. 2.16	[41, 42]
Immune system	$\begin{cases} \frac{dT}{dt} = f(T) - f(I) \cdot T \cdot \left(\frac{h}{T+h}\right) \\ f(I) = d \cdot I \end{cases}$	Eq. 2.17	[44]
	$\begin{cases} \frac{dT}{dt} = f(T) - f(I) \cdot T \cdot \left(\frac{h}{T+h}\right) \\ f(I) = (d_1 \cdot I_1 + d_2 \cdot I_2) \cdot \left(\frac{I_3}{I_3 + g}\right) \end{cases}$	Eq. 2.18	[43]
	$\frac{dT}{dt} = f(T) - d_1 \cdot I \cdot T - d_2 \cdot N \cdot T$	Eq. 2.19	[46]
	$\frac{dT}{dt} = f(T) - d \cdot I \cdot T$	Eq. 2.20	[47]
Empirical model structures describing therapeutic effect			
First-order treatment effect ("log-kill" pattern)	$\frac{dT}{dt} = f(T) - k_d \cdot T$	Eq. 2.21	[18]
Exposure-dependent treatment effect	$\frac{dT}{dt} = f(T) - k_d \cdot Exposure \cdot T$	Eq. 2.22	[22, 25]

Table 2.1 continues on next page.

Table 2.1: *Continued*

Models/assumptions	Equations		Ref.
Exposure-dependent treatment effect with resistance (TGI model)	$\frac{dT}{dt} = f(T) - k_d \cdot e^{-\lambda \cdot t} \cdot Exposure \cdot T$	Eq. 2.23	[20, 48, 49]
Introducing a damaged cell compartment	$\begin{cases} \frac{dS}{dt} = f(S) - k_d \cdot Exposure \cdot S \\ \frac{dD}{dt} = k_d \cdot Exposure \cdot S - d \cdot D \\ T = S + D \end{cases}$	Eq. 2.24	[24, 25]
Nonlinear drug exposure-effect relationship	$k_g{}' = k_g \cdot \left(1 - \frac{E_{max} \cdot Exposure}{IC_{50} + Exposure}\right)$	Eq. 2.25	[21]
Algebraic equations			
Two-phase model	$T = \left(e^{-k_d \cdot t} + e^{k_g \cdot t} - 1\right) \cdot BASE$	Eq. 2.26	[50, 51, 55]
	$T = \left(e^{-k_d \cdot t} + e^{k_g \cdot (t-\tau)} - 1\right) \cdot BASE$	Eq. 2.27	[50]
	$T = \left(\phi \cdot e^{-k_d \cdot t} + \left[e^{k_g \cdot t} - \phi\right]\right) \cdot BASE$	Eq. 2.28	[55]
Model proposed by Wang et al.	$T = BASE \cdot e^{-A \cdot t} + B \cdot t$	Eq. 2.29	[52, 56]
An extension of Eq. 2.30	$T = BASE \cdot e^{-A \cdot t} + B \cdot t + C \cdot t^2$	Eq. 2.30	[53]
	$A = \theta_1 + \theta_2 \cdot \left(\frac{Dose}{100mg}\right)$	Eq. 2.31	[53]
Simplified TGI model	$T = BASE \cdot e^{k_g \cdot t - \left(\frac{k_d}{\lambda}\right) \cdot \left(1 - e^{-\lambda \cdot t}\right)}$	Eq. 2.32	[54, 57, 58, 59, 60]
Partial differential equations			
Proliferation-invasion model	$\frac{\partial c(x,t)}{\partial t} = Diff \cdot \nabla^2 c(x,t) + f\left(c(x,t)\right)$	Eq. 2.33	[61, 63, 64, 69, 70]
	$v = 2\sqrt{Diff \cdot \rho}$	Eq. 2.34	
	$\frac{\partial c(x,t)}{\partial t} = Diff \cdot \nabla^2 c(x,t) + f\left(c(x,t)\right) - k_d \cdot c(x,t)$	Eq. 2.35	[67]
	$Surv = e^{-(\alpha \cdot Dose + \beta \cdot Dose^2)}$	Eq. 2.36	[64]

Table 2.1 continues on next page.

Table 2.1: *Continued*

Models/assumptions	Equations		Ref.
Proliferation-invasion model	$\frac{\partial c(x,t)}{\partial t} = Diff \cdot \nabla^2 c(x,t) + f\big(c(x,t)\big) - (1 - Surv) \cdot f\big(c(x,t)\big)$	Eq. 2.37	[64]
	$\frac{\partial c(x,t)}{\partial t} = Diff \cdot \nabla^2 c(x,t) + f\big(c(x,t)\big) - G(x,t)$	Eq. 2.38	[74]

a, β, radio sensitivity parameters; *A*, exponential shrinkage rate constant as a result of treatment; *a, b,* constants; *B*, linear growth rate constant; *BASE*, baseline of tumor burden; BM_0, baseline of biomarkers; BM_t, biomarker amount at time point t, which could be assumed to remain constant and equal to baseline in the absence of treatment; *C,* coefficient of quadratic growth term; *c(x,t),* tumor cell concentration/density at location x at time t; *D*, damaged cells; *d*, death rate constant; d_1, d_2, rate constants; *Dif*, diffusion coefficient; *E*, vessel endothelial cells; E_{max}, maximal fraction of inhibition; *f(P), f(S), f(R), f(T),* growth function of proliferative cells (P), sensitive cells (S), resistant cells (R), and tumor tissue (T), respectively; *G*(*x,t*), surgical term; *h, g*, constants; *I*, I_1, I_2, I_3, components in the immune system; IC_{50}, the drug exposure that produces 50% of E_{max}; *k*, k_2, rate constants; k_d, shrinkage rate constant of tumor as a result of drug treatment; k_g, growth rate/growth rate constant; k_g', tumor growth rate constant under treatment; m_1, m_2, conversion rate constants that can be set as 0; *N*, normal cells; *Surv*, the probability of tumor cell survival; *T*, tumor burden; TGI, tumor growth inhibition; T_{max}, carrying capacity; *λ*, treatment efficacy decay rate constant; λ_0, exponential growth rate; λ_1, linear growth rate; *τ*, delayed time of tumor regrowth; *ϕ*, sensitive fraction of the tumor; *ρ*, growth rate constant; ∇^2, a Laplacian operator; *f(c(x,t))*, tumor proliferation function.

The exponential growth assumes the growth rate of a tumor is proportional to tumor burden (first-order growth; Eq. 2.3; **Figure 2.1**) [10, 19]. It has been adopted in a widely used tumor growth inhibition (TGI) model developed by Claret et al. to describe nature tumor growth [11, 20].

The linear and exponential growth models have also been expanded by introducing a first-order shrinkage term describing natural tumor death. For example, a model with a linear growth and a first-order shrinkage (Eq. 2.2) was applied to describe the natural tumor growth in patients with advanced solid malignancies based on SLD measurements [21]. An exponential growth with a first-order shrinkage (Eq. 2.4) was also used as part of the model structure to describe the natural growth of pediatric neuroblastoma based on tumor volume measurements [22]. The same model structure was also adopted for the description of the change of prostate cancer burden reflected by the level of prostate-specific antigen (PSA) [23].

When compared with the unlimited growing pattern of linear and exponential growth models, the logistic and Gompertz growth models provide a biologically realistic change of the growth rate as the tumor burden increases [6] (**Figure 2.1**). The logistic growth model assumes that the growth is limited by a carrying capacity (Eq. 2.5) [10] whereas the Gompertz model assumes the growth rate of tumor decreases over time (Eqs. 2.6 and

2.7) [10, 11]. Many clinical studies have applied the logistic [24-26] and Gompertz models [11, 27] as well as simulation studies [28, 29].

Finally, a combination of exponential and linear growth models (Eq. 2.8) has also been introduced to describe tumor growth in patients, although it was proposed primarily for characterizing xenograft tumor dynamics [30]. This combined model structure assumes that an exponential (first-order) growth switches to a linear (zero-order) growth after reaching a threshold (**Figure 2.1**). It was well used to describe the natural growth of vestibular schwannoma volume in patients with neurofibromatosis type 2 [31]. Setting the power term as 20 allows the switch between two growth patterns sharply enough [30].

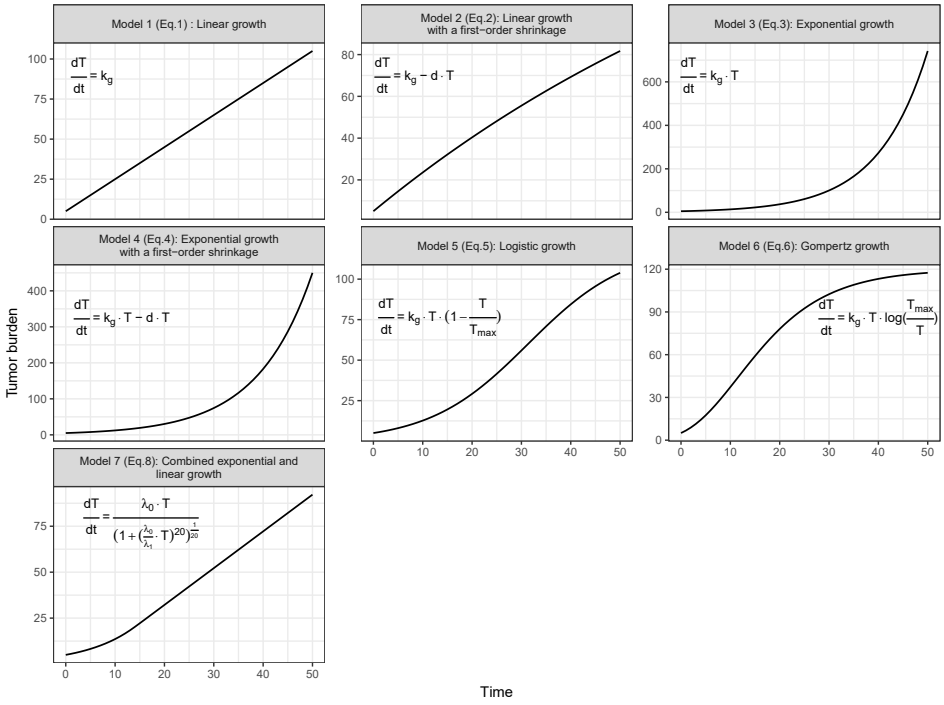

Figure 2.1: Simulated time curves of tumor burden (*T*) with tumor natural growth models displayed by Eqs. 2.1–2.6 and 8. *kg* is the tumor growth rate / growth rate constant, *d* is the tumor death rate constant, T_{max} is the carrying capacity, λ_0 is the exponential growth rate, and λ_1 is the linear growth rate. The baseline of tumor burden is 5. Parameter values used for the simulations are as follows: Models 1 and 2 (Eqs. 2.1 and 2.2), *kg* = 2; Model 2 (Eq. 2.2), *d* = 0.01; Models 3–6 (Eqs. 2.3–2.6), *kg* = 0.1; Model 4 (Eq. 2.4), *d* = 0.01; Models 5 and 6 (Eqs. 2.5 and 2.6), T_{max} = 120; Model 7 (Eq. 2.8), λ_0 = 0.1, λ_1 = 2.

3.1.2 Tumor heterogeneity

As a result of the increasing awareness of the relevance of considering tumor heterogeneity, model structures displayed by ODEs that incorporate tumor heterogeneity and mutations have been developed for the characterization of tumor dynamics as was described in a simulation study [32]. The general used model structures concerning tumor heterogeneity are shown in **Table 2.1**.

Proliferative and quiescent cells

One frequently made assumption when modeling the growth of heterogeneous tumors is to separate total tumor mass into proliferative and quiescent cells [22, 25, 33]. The increase of quiescent tumor cells is assumed to result from a first-order conversion from proliferative tumor cells instead of their own proliferation (Eq. 2.9). A reversed conversion can also be assumed to be present (Eq. 2.10). The growth of proliferative cells may follow the patterns as were introduced in the Basic growth model section Based on these assumptions, the time courses of mean tumor diameter (MTD) in patients with low-grade glioma [25] and that of tumor volume in pediatric neuroblastoma patients were successfully described [22]. A similar model structure was also used to predict the effect of different treatment regimens taking tumor cell number as a target [33]. Drug treatment effect could work on both kinds of tissues [25], only on the proliferative tissue [22], or on targeted tissues depending on the types of drug [33].

Sensitive and resistant cells

Another commonly made assumption is that tumors are composed of drug-sensitive and drug-resistant cells [24, 34]. These two cell types both proliferate, but drug treatment can only decrease the amount of drug-sensitive cells. Primary and acquired resistance can both be taken into consideration. For illustrating the acquired resistance, the resistant cells are mostly assumed to mutate from sensitive cells because of the treatment with a first-order process [23, 24, 34, 35] (Eqs. 2.12–2.13). By separating tumor mass into sensitive and resistant cells, the dynamics of low-grade glioma measured with MTD in patients was well described with models assuming that primary resistant cells or both primary and acquired resistant cells are present in the tumor [24]. In the study, the natural growth of drug-sensitive and primary-resistant cells were described separately without any conversion (Eq. 2.11). The acquired resistant cells are assumed to emerge exponentially from damaged sensitive cells as a result of treatment. Also, by assuming that resistant cells can also convert back to sensitive cells (Eq. 2.13), the dynamics of the PSA level in prostate cancer patients was well described, where the rate constants of cell proliferation, apoptosis, and conversion are expressed as functions of intracellular concentration of androgen receptors [34].

In addition, the treatment sensitivity of both proliferative and quiescent cells can also be considered when modeling tumor growth, leading to a combination of previous introduced model structures. One example can be seen from a study that assumed proliferative and quiescent cells form a tumor and the proliferative cells could mutate from drug sensitive to drug resistant, which is biologically plausible [33].

Androgen-dependent cells and androgen-independent cells

Studies regarding prostate cancer often consider prostate tumors consists of androgen-dependent (AD) and androgen-independent (AI) cells [23, 36-38]. PSA levels are commonly used to represent tumor burden in this case. Two frequently reported model structures for describing the growth of prostate cancer were proposed by Ideta et al. [23] and Hirata et al. [36].

The former model structure assumes that prostate cancer consists of AD and AI cells, and AD cells can mutate exponentially to AI cells when treatment alters the androgen level. The model structure is shown in Eq. 2.12. The natural proliferation and apoptosis rate constants of AD and AI cells were expressed as functions of the androgen level [23]. The net growth rate of AD decreases when the androgen level decreases because of treatment, whereas that of AI cells increases. When the androgen level is normal, three cases of the net growth rate of AI cells were considered: larger than 0, equal to 0, and smaller than 0. This model was recently extended by accounting for competition between two kinds of cells and the finite carrying capacity environment [35].

The latter model structure assumes that besides AD cells, reversible and irreversible AI cells exist. All types of cells are assumed to proliferate and convert to each other exponentially. It is assumed that AD cells convert to both types of AI cells during on-treatment status and reversible AI cells convert back to AD cells during off-treatment status. The model structure is expressed with Eq. 2.13. This model has been applied to adequately describe patient data [37, 38].

3.1.3 Integration of biology process

Tumor growth models displayed by ODEs that additionally incorporate biological factors and processes have also been developed [6], such as integration of angiogenesis biomarkers and the dynamics of components in the immune system (**Table 2.1**). To apply these methods, apart from tumor burden measurements, knowledge related to the biological processes is also needed.

Angiogenesis

Concentration of vascular endothelial growth factor (VEGF) or soluble VEGF receptor may serve as biomarkers indicating the treatment effect for patients treated with angiogenesis inhibitors [11]. Incorporating the dynamics of angiogenesis biomarkers in tumor growth modeling enables better understanding and prediction of tumor progression. A model structure showed as Eq. 2.14, where the change of biomarkers from baseline affects the tumor decay rate, was applied in two studies [31, 39]. One study characterized the time course of SLD in patients with gastrointestinal stromal cancer undergoing sunitinib treatment. The natural growth of the tumor was described with the exponential model, and the model-predicted relative change of the biomarker's amount was incorporated to affect the shrinkage of the tumor [39]. The other study well characterized the dynamics of tumor volume measured in neurofibromatosis patients undergoing bevacizumab and everolimus. The natural tumor growth was described by the combined exponential and linear model (Eq. 2.8), and the amount of unbound VEGF was considered to affect a first-order apoptosis of the tumor [31].

Another way to account for angiogenesis effect on tumor growth is by assuming the carrying capacity of the tumor is determined by the effective tumor vascular support that is in turn affected by the tumor volume (Eqs. 2.15 and 2.16) [40, 41]. Logistic and Gompertz model structures were applied under this assumption. A model structure displayed by Eq. 2.15 was applied to well characterize the tumor growth in renal cell carcinoma (RCC) patients based on SLD measurements [40]. The carrying capacity in this study was assumed to expand because of proangiogenic factors. Another similar model structure is shown by Eq. 2.16. Although as far as we know there is no clinical study that utilized this model framework, it has been used to perform simulations to optimize the delivery of therapeutic agents for enhancing targeted therapies for liver cancer [41] and to investigate the optimization of antiangiogenic treatment [42].

Immune system

Apart from angiogenesis, the effect of the immune system has also been incorporated in the tumor growth model when patients were undergoing immunotherapy [43, 44]. The proposed model structure is presented in Eqs. 2.17 and 2.18, where the rate of first-order decline of tumor burden was assumed to depend on the amount of immune component and decrease while tumor burden was increasing. This model structure was adopted to characterize the growth of prostate cancer by accounting for the dynamics of the immune system. Tumor cells were assumed to proliferate exponentially, and the amount of cytotoxic T lymphocytes affected the cell decline rate (Eq. 2.17) [44]. The applicability of this model was validated by the results of a clinical trial where PSA measurements were obtained from

prostate cancer patients treated with a vaccine. Considering the effect of more than one immune component, another study developed a model structure to simulate the growth of bladder cancer undergoing immunotherapy [43]. The growth of tumor cells was described with a logistic model, and the cell decline rate was set to be linearly or nonlinearly related to the amount of immune components (Eq. 2.18).

Another concept model structure described tumor burden dynamics by a logistic growth, a first-order damage resulting from immune cells, and a first-order competition with normal cells (Eq. 2.19) [45]. This model structure was recently adopted to obtain an optimal dosing regimen for cancer patients based on simulation [46]. A model structure that omits the competition with normal cells (Eq. 2.20) was also proposed to investigate treatment optimization [47].

3.1.4 Treatment effect

Empirical method

Tumor shrinkage resulting from drug treatment is typically quantified with an empirical drug-induced shrinkage term as has previously been summarized [10]. Commonly used equations identified from included papers are presented in **Table 2.1**. The time curves of these equations were simulated with R and are shown in **Figure 2.2**, assuming an exponential growth with the growth rate constant $k_g = 0.1$.

A log-kill pattern is commonly used for modeling treatment effect, which assumes that the shrinkage rate of the tumor as a result of drug treatment is proportional to tumor burden [6]. The simplest way to adopt this pattern is using Eq. 2.21, where k_d is the drug-induced tumor shrinkage rate constant. Such an equation has been used to well described the treatment effect of everolimus on metastatic RCC patients [18]. The estimates of k_d in that study were different between two dose groups.

The rate of drug-induced shrinkage can also be considered to depend on drug exposure, i.e., drug concentration and area under the concentration-time curve or drug dose. A linear drug exposure-effect relationship can be quantified using Eq. 2.22 [22, 25]. Meanwhile, drug resistance can also be taken into consideration by introducing a $e^{-\lambda \cdot t}$ term on the basis of Eq. 2.22 to quantify the decline of drug effect over time (Eq. 2.23; **Figure 2.2**). This model structure has been applied to characterize the effect of pazopanib on RCC patients [40]. Setting $f(T) = k_g \cdot T$, an exposure-driven TGI model was developed based on SLD measurements from colorectal cancer patients receiving capecitabine and fluorouracil [20]. It has then been widely applied to various cancer types and drugs as was reviewed previ-

ously [11]. Two more recent studies also adopted this model structure to characterize the tumor SLD change in metastatic breast cancer patients treated with eribulin [48] and in metastatic ovarian cancer patients receiving carboplatin or gemcitabine plus carboplatin [49], respectively.

In addition, a damaged cell compartment (*D*) has also been introduced in studies to account for the damage on cell DNA as a result of the treatment, as is displayed by Eq. 2.24, which can result in a delay on drug onset (**Figure 2.2**). This model structure was used in two studies that characterized the MTD change in low-grade glioma patients treated with chemotherapy or radiotherapy [24, 25]. In these two studies, the damaged cell compartment was used to characterize the treatment effects on drug-sensitive cells [24] and quiescent cells [25] respectively. Part of the damaged cells eventually died, and the rest were assumed to become drug-resistant cells [24] and proliferative cells [25] respectively.

Apart from the linear drug exposure-effect relationship, a nonlinear drug exposure-effect relationship can also be considered to characterize treatment effect particularly for targeted anticancer treatment [21]. An E_{max} model is commonly used in this circumstance. An example equation is showed as Eq. 2.25, which was derived from a model where the studied medicine was assumed to inhibit the zero-order growth rate of advanced solid malignancies following the nonlinear drug exposure-effect relationship [21].

Considering biomarkers

When biomarkers that represent the drug-targeting system are incorporated in the tumor dynamic models, treatment effect can be added on the dynamics of biomarkers according to corresponding mechanisms.

In the study where neurofibromatosis patients were treated with bevacizumab and everolimus, the decrease of the unbound VEGF amount because of the binding with bevacizumab was considered in the model [31]. Meanwhile, the inhibition of the zero-order production rate of total VEGF because of everolimus was described with a nonlinear exposure-effect relationship: $k^{'} = k \cdot \left(\frac{IC_{50}}{IC_{50} + Exposure}\right)$, where IC_{50} the drug exposure that produces 50% of the maximal inhibition effect. As a result of the quantity decrease of biomarkers, the shrinkage rate of tumor burden increased (Eq. 2.14). The delayed activation of tumor proliferation result from the continuous use of everolimus was also integrated in their model structure [31]. In the study where gastrointestinal stromal cancer patients were treated with sunitinib, the effect of sunitinib was described by a nonlinear inhibition on the zero-order production rate or first-order decline rate of biomarkers using $k^{'} = k \cdot \left(1 - \frac{I_{max} \cdot Exposure}{IC_{50} + Exposure}\right)$, where Imax is the maximal fraction of inhibition

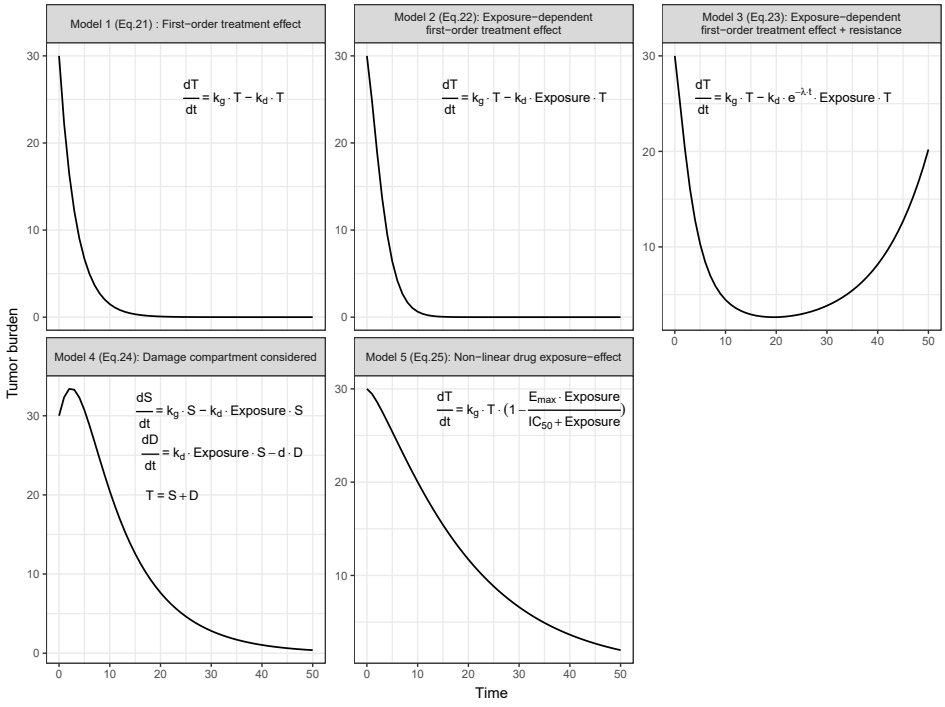

Figure 2.2: Simulated time curves of total tumor burden (T) with tumor dynamic models incorporating treatment effect with Eqs. 2.21–2.25 and assuming an exponential growth (growth rate constant $kg = 0.1$). k_d is the tumor shrinkage rate constant due to drug treatment, λ is the treatment efficacy decay rate constant, *S* is the drug sensitive cells, *D* represents the damaged cells, *d* is the death rate constant. E_{max} is the maximal fraction of inhibition, and IC_{50} is the drug exposure that produces 50% of E_{max}. The baseline of total tumor burden is 30. Parameter values used for the simulations are as follows: Model 1 (Eq. 2.21), $k_d = 0.4$; Models 2–4 (Eqs. 2.22–2.24), $k_d = 0.04$; Model 3 (Eq. 2.23), $\lambda = 0.1$; Model 4 (Eq. 2.24), $d = 0.1$; Model 5 (Eq. 2.25), $E_{max} = 2$, $IC_{50} = 5$. Drug exposure was simulated with Hill's equation: $Exposure = Ep_{max} \cdot \frac{t^{0.5}}{Ept_{50}{}^{0.5} + t^{0.5}} = 30 \cdot \frac{t^{0.5}}{10^{0.5} + t^{0.5}}$, where Ep_{max} represents the maximum exposure at steady state and Ept_{50} represents the time when the exposure reaches half maximum value.

[39]. The negative item in Eq. 2.23 was also included to quantify the treatment effect and resistance [39].

In addition, the effect of angiogenesis inhibition treatment can also be incorporated by introducing a first-order drug exposure dependent decline term (Eq. 2.22) on the dynamics of tumor vascular support [40, 41] when the vascular support was assumed to determine the carrying capacity of tumor (Eqs. 2.15 and 2.16).

Studies where patients were treated with immunotherapy have also considered drug interaction with the immune system. The presence of immunotherapeutic agents is frequently assumed to affect the dynamics of components in the immune system, and the amount of

those components can affect the decrease rate of tumor burden (Eqs. 2.17 and 2.18) [43, 44]. For example, the model structure proposed to describe PSA change in prostate cancer patients treated with a vaccine assumed that the presence of the vaccine upregulated the zero-order production rate of mature dendritic cells and therefore increased the number of cytotoxic T lymphocytes, which increased the decay of tumor tissue [44].

3.2 Algebraic equation

Besides using ODEs, model structures displayed by algebraic equations have also been developed to characterize the dynamics of tumor directly as is summarized in **Table 2.1** [50-54]. The simulated time curves of tumor dynamics given by these models are shown in **Figure 2.3**. Although these equations could be treated as analytical solutions of ODEs, they provided different shapes of time curves when compared with what was introduced previously.

A novel two-phase model that combines exponential tumor regrowth and regression was developed to interpret serial PSA measurements from AI prostate cancer patients [50] and metastatic castration-resistant prostate carcinoma patients undergoing combination therapy [51]. The corresponding model equation is shown in Eq. 2.26, where k_g is the tumor regrowth rate constant and k_d is the drug-dependent tumor regression rate constant. The same model structure was also utilized to assess the therapeutic efficacy of bevacizumab in patients with RCC using the sum of perpendicular diameter measurements [55]. On the bases of this model structure, an extra parameter τ has been introduced to account for the delayed tumor regrowth as presented in **Figure 2.3** (Eq. 2.27) [50]. In addition, a parameter ϕ has also been introduced on the basis of Eq. 2.26 to differentiate the sensitive and resistant part of the tumor (Eq. 2.28) [55], which results in a less degree of tumor shrinkage at the early phase (**Figure 2.3**). This model structure was found to be applicable when sufficient data points were available, and the estimation of growth rate constant was similar to what was obtained by the original equation (Eq. 2.26).

Another model structure was proposed by Wang et al. to describe the time courses of tumor SLD data of non-small cell lung cancer (NSCLC) patients from four clinical trials treated with eight treatments/placebos [11, 52], as shown by Eq. 2.29. A and B represent the rate constants of exponential shrinkage as a result of treatment and linear growth, respectively. The treatment effect was also characterized as a drug-dependent manner. This model structure has been successfully applied afterward [11] and was recently applied to analyze SLD measurements collected from NSCLC patients from three clinical studies to identify the obstacles to wider use of quantitative measures [56].

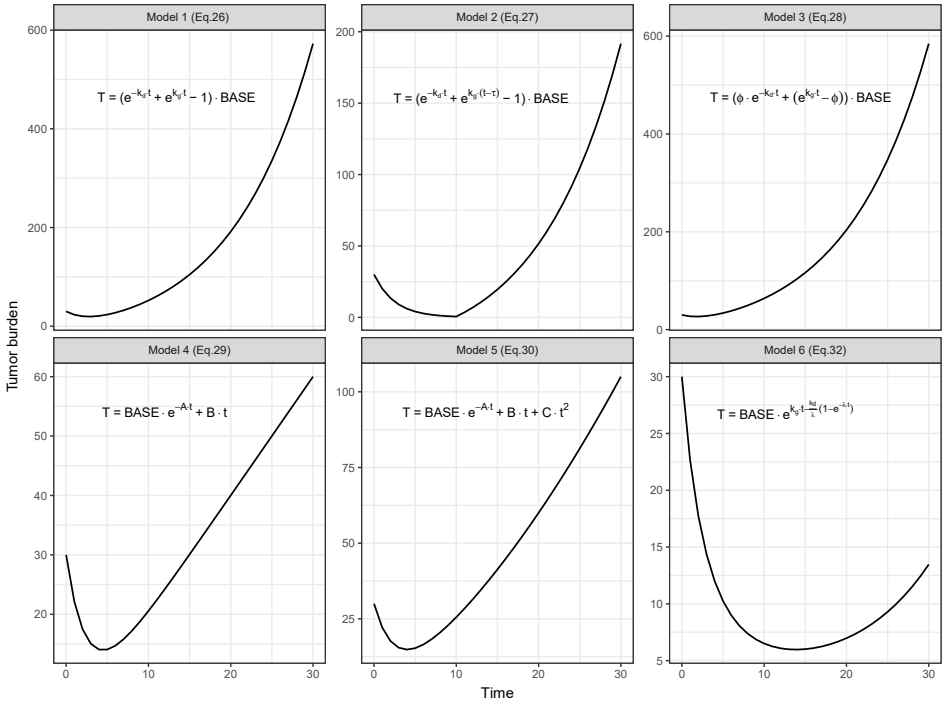

Figure 2.3: Simulated time curves of tumor burden (*T*) with tumor dynamic models displayed by algebraic equations that describe both tumor natural growth and treatment effect (Eqs. 2.26–2.30 and 2.32). k_g is the tumor growth rate constant, k_d is the tumor shrinkage rate constant due to drug treatment, τ is the delayed time of tumor regrowth, ϕ is the sensitive fraction of the tumor, *A* is the exponential shrinkage rate constant due to treatment, *B* is the linear growth rate constant, *C* is the coefficient of quadratic growth term, *BASE* is the baseline of tumor burden, and λ is the treatment efficacy decay rate constant. Parameter values used for the simulations are as follows: Models 1–3 (Eqs. 2.26–2.28), $k_g = 0.1$, $k_d = 0.4$, *BASE* = 30; Model 2 (Eq. 2.27), τ = 10; Model 3 (Eq. 2.28), $\phi = 0.6$; Models 4 and 5 (Eqs. 2.29 and 2.30), $A = 0.4$, $B = 2$, $C = 0.05$, *BASE* = 30; Model 6 (Eq. 2.32), $k_g = 0.1$, $k_d = 0.4$, $\lambda = 0.1$.

A quadratic growth term with a coefficient *C* was later introduced to this model structure as is shown in Eq. 2.30 [53]. This model structure was demonstrated to have the best performance on characterizing the SLD measurements in RCC patients receiving pazopanib or placebo, and predictive patient-specific covariates were also identified [53]. Treatment effect, which is reflected by parameter *A*, was described in a dose-depended manner for one group of the patients in this case (Eq. 2.31).

In addition, a simplified version of the previously introduced TGI model, which was displayed by an algebraic equation, was also developed (Eq. 2.32) [54]. This model structure also assumes an exponential tumor growth with growth rate (k_g) while the treatment effect is described in a drug-dependent manner with parameters account for tumor growth inhibition (k_d) and drug resistance (λ). By applying this model structure, the tumor size

change in metastatic colorectal cancer patient treated with bevacizumab and chemotherapy was described satisfactorily [54]. This model structure has been well applied to describe tumor size change in metastatic RCC patients treated with cytokine, mammalian target of rapamycin inhibitor, and VEGF receptor inhibitors [57]; in NSCLC patients undergoing treatment of carboplatin/paclitaxel combining motesanib or not [58]; in NSCLC patients treated with bevacizumab and erlotinib [59]; and in gastric cancer patients treated with bevacizumab and chemotherapy [60].

3.3 Partial differential equation

3.3.1 Natural growth

Partial differential equations (PDEs), which take the change of a dependent variable in time and space into consideration, have also been adopted in the modeling of solid tumor dynamics in clinical research. One common application is known as a proliferation-invasion model or a reaction-diffusion model, which hypothesize that it is the net proliferation and invasion that contribute to the growth of cancer [61]. This model formation has been typically used in studies where imaging observations of tumor, especially brain tumors, were available to describe and predict tumor expansion [8]. The equation of this structure is shown as Eq. 2.33 in **Table 2.1**, where the dynamics of tumor cell concentration/density at location x at time t ($c(x, t)$) is described [8, 61]. The tumor proliferation in this model can be expressed by exponential, logistic, or Gompertz functions [8, 61]. Moreover, this model mathematically regards the expansion of imaging detectable tumor edge as a "traveling wave," and the velocity of tumor expansion is a constant that is determined by the diffusion coefficient (*Dif*) and growth rate constant ρ (Eq. 2.34) [61]. This linear radius/ diameter expansion was confirmed in a group of grade II gliomas patients with magnetic resonance image (MRI) measurements before any oncological treatment [62].

Studies applying the proliferation-invasion model to characterize tumor dynamics typically have interest in estimating the rate constants of net proliferation and invasion. An application of this model structure can be found in a study where the tumor volumes obtained from the MRI imaging were available for 70 patients with previously untreated glioblastoma [61]. The tumor proliferation was described by a logistic function (Eq. 2.5) with a growth rate constant ρ. The ratio Dif / ρ was estimated for each patient based on MRI observations. Subsequently, setting ρ as a reported mean value and estimating *Dif*, the velocity of tumor radial expansion was estimated, and the survival time of patients underwent tumor resection were satisfactorily predicted by the estimated time of reaching a target radius. The same model structure was also applied on serial available MRI data

from 32 glioblastoma patients before treatment [63]. The net proliferation and invasion rates they quantified were significantly associated with the survival of patients. Another study characterized tumor natural growth for nine patients with glioblastoma with the same model [64]. This study demonstrated that the parameter estimated based on pretreatment MRIs had high prediction accuracy for responses after treatment for these patients. Using the same model structure, the correlation between proliferation rate and hypoxic volumes based on imaging data from newly diagnosed glioblastomas patients was demonstrated [65]. This model structure was also recently used to investigate the personalization of radiotherapy strategy for brain cancer patients [66].

Setting $f(c(x,t)) = \rho \cdot c(x,t)$ a similar model structure was also used to simulate the growth of glioblastoma based on previous reported parameters estimated from patients and estimated the survival times of patients under different parameter settings [67].

Likewise, the proliferation-invasion model with logistic growth function was also successfully applied in breast cancer patients to characterize and predict their tumor burden. [68] The model developed based on MRI data that were available from the early treatment phase was demonstrated to be able to predict patient response at the end of treatment [69, 70]. In these studies, an apparent diffusion coefficient was estimated based on diffusion-weighted MRI data and was then transformed to an estimate of tumor cell number, which was the dependent variable in the model. Moreover, the inhibitory effect of tumor diffusivity resulting from the stress and the deformation of surrounding tissue forced by the tumor cells were also considered in these studies [69, 70], which is called "mass effect" [8]. More examples of the application of the proliferation-invasion model can be found in a previous review [8].

Apart from taking the diffusion coefficient as a constant, the difference between diffusion rates in gray and white matter can also be considered, such as setting *Dif* as two different constants for the cells in gray and white matter, respectively [71]. The proportions of white and gray matter (i.e. $P_w(x)$, $P_g(x)$) have also been taken into account when computing the diffusion coefficient with the following equation: $Dif(x) = P_g(x) \cdot Dif_g + P_w(x) \cdot Dif_w$. The prediction of the model was validated with clinical imaging data from one glioma patient case [72].

Recently, a threshold and a necrosis rate were also introduced into the proliferation-invasion model structure, which assumes an exponential decay will occur once the tumor cell amount exceeds the threshold [73].

3.3.2 Treatment effect

When using the proliferation-invasion model, the treatment effect can also be expressed by subtracting an extra term (corresponding equations are shown in **Table 2.1**). The effect of chemotherapy can be expressed with Eq. 2.35, where k_d is the drug effect rate constant [67]. For radiotherapy, a linear-quadratic equation has been used to estimate the probability of tumor cell survival (*Surv*) after the administration of radiation with dose (*Dose*) (Eq. 2.36). The effect of radiotherapy can thus be incorporated as presented by Eq. 2.37 [64]. In addition, it is also possible to incorporate the effect of resection in the proliferation-invasion model to describe tumor growth after surgery. The resection can be simulated by setting the cell concentration in the resected region as zero at the time point of surgery [61]. Subtracting a surgical term (Eq. 2.38) was also found to be applied to simulate the resection of tumor [74].

4. Tumor resistance evolution modelling

4.1 Tumor clonal evolution

Theoretically, three models of tumor evolution have been reported. One is a selective sweep model, which is also known as "linear" model [14, 75]. It holds that during cancer initiation, mutations with fitness advantage are raised and then selectively take over the whole population sequentially [14, 75]. However, because intratumor heterogeneity was identified and evidence of branching growth was found from multibiopsy and genomewide studies, a branching evolution theory where multiple subclones are considered to present and compete was developed [14, 75]. Another "big bang" model of tumor evolution was observed in colorectal tumors, which suggests that advantage mutations arise and cumulate during the early phase of cancer development and the tumor then grows as a neutral single clonal [14, 75].

Mathematical models that characterize tumor initiation and progression as an evolving process, including stochastic models and deterministic models, were sufficiently introduced in previous reviews [13, 14]. A well-mixed cell population is typically assumed [13]. Modeling strategies that focus on describing the evolution of cancer resistance have also been discussed [15, 17]. In the following sections, we will mainly give an introduction about different mathematical modeling strategies that were used to characterize cancer resistance with the tumor evolution principle.

4.2 Stochastic model

4.2.1 Probability model assuming the branching process

The branching process, which is also called the birth-death process, is a commonly adopted stochastic process that is used to characterize the evolving dynamics of cancer resistance [13, 15, 17]. The Markov property is adopted in this model. Normally, at least two cell types, i.e., sensitive cells and resistant cells, are considered. It assumes that a tumor grows exponentially and that each sensitive cell has a certain birth rate, death rate, and a mutation probability in one cell division, and each resistant cell also has a certain birth rate and death rate. The probability of cell number change from current generation to the next could therefore be expressed with these parameters, as is shown in Eq. 2.39 (**Table 2.2**). *n* and *m* the numbers of sensitive cells and resistant cells, respectively. Substantially, stochastic simulation could be performed and the probability of resistance (the probability of at least one resistant cell is present; P_R) and the expected number of resistant cells (E_R) could be calculated with probability-generating function.

Resistance evolution before treatment

By applying the branching process, the resistance evolution before treatment can be investigated. One study estimated the P_R and E_R of a cell population reached a certain size through the branching process starting with one sensitive cell [76]. The fitness of the resistant cells that is relative to sensitive cells was also taken into consideration [76]. The derived equations were later adopted to estimate the resistance probability of colorectal cancer prior to endothelial growth factor receptor (EGFR) antibody treatment, where the parameters were estimated based on longitudinal *KRAS* mutation amount measurements [77]. The results indicated that the resistant mutation was highly likely to be present prior to the initiation of treatment. The same process has also been applied to investigate the evolution of drug resistance in chronic lymphocytic leukemia before treatment [78], where the growth and death rates of cancer cells were set based on patient results. In this case, besides estimating P_R and E_R at the time of treatment start, a time needed for the resistant population to reach a detectable level after treatment was also estimated based on which disease progression was analyzed and compared with real patient data.

Another study proposed functions for estimating the expected and median cell numbers for each resistant subclone in a metastatic lesion containing a certain number of cells with the branching process starting with a single sensitive cell [79]. The predictions of relative cell numbers of resistant subclones assuming resistant cells were neutral were demonstrated to be in agreement with what was estimated based on the mutation concentrations in circulation tumor DNA (ctDNA) obtained from colorectal cancer patients treated with an EGFR blockade [79].

Table 2.2: Modeling frameworks for characterizing tumor resistance evolution

Models	Equations		Ref.
Stochastic models			
Probability model assuming branching process	$\begin{cases} P(n+1,m\|n,m) = b_s \cdot (1-u) \cdot n \cdot \Delta t \\ P(n-1,m\|n,m) = d_s \cdot n \cdot \Delta t \\ P(n,m+1\|n,m) = b_r \cdot m \cdot \Delta t + b_s \cdot u \cdot n \cdot \Delta t \\ P(n,m-1\|n,m) = d_r \cdot m \cdot \Delta t \\ P(n,m\|n,m) = 1 - \left((b_s + d_s) \cdot n \cdot \Delta t + (b_r + d_r) \cdot m \cdot \Delta t\right) \end{cases}$	Eq. 2.39	[76, 81, 83]
Stochastic differential equation	$\begin{cases} dS = k_g \cdot S \cdot \left(1 - \frac{(S+R)}{T_{max}}\right) \cdot dt - u \cdot S \cdot dt - k_d{}' \cdot S \cdot dt + \sigma_1 \cdot S \cdot dW_1 - q_M \cdot K \cdot S \cdot dN_1 \\ k_d{}' = k_d \cdot \frac{C_D}{K_D + C_D} \end{cases}$	Eq. 2.40	[90]
Deterministic models			
Ordinary differential equation	$\begin{cases} \frac{dS}{dt} = \left(k_g - d - k_d\right) \cdot S \\ \frac{dR}{dt} = \left(k_g - d\right) \cdot R + u \cdot S \end{cases}$	Eq. 2.41	[91]
	$\begin{cases} \frac{dS}{dt} = \left(k_g \cdot (1-u) - d - k_d\right) \cdot S \\ \frac{dR}{dt} = \left(k_g - d\right) \cdot R + k_g \cdot u \cdot S \end{cases}$	Eq. 2.42	[88]
	$\begin{cases} \frac{dS}{dt} = \left(k_g - k_d \cdot Dose\right) \cdot S \\ \frac{dR}{dt} = k_g \cdot R + k_g \cdot u \cdot S \end{cases}$	Eq. 2.43	[92]
	$\begin{cases} \frac{dS}{dt} = \left(k_{g1} - u_1 - k_{d1} \cdot C_D\right) \cdot S + u_2 \cdot R \\ \frac{dR}{dt} = \left(k_{g2} - u_2\right) \cdot R + u_1 \cdot R \end{cases}$	Eq. 2.44	[93]
Game theory	$W(i) = \sum p_j \cdot Payoff(ij) = 1 - r_i - d_i + (1 - p_i) \cdot X_i$	Eq. 2.45	[94]
	$\overline{W} = \sum p_i \cdot W(i)$	Eq. 2.46	
	$\frac{dp_i}{dt} = p_i \cdot (W(i) - \overline{W})$	Eq. 2.47	
Integral-differential equation	$\begin{cases} \frac{\partial n(x,t)}{\partial t} = \left[r(x) \cdot (1-\theta) - c(x) - G(\rho(t)) \cdot d(x)\right] \cdot n(x,t) + \theta \cdot \int_0^1 r(y) \cdot M(y,x) \cdot n(y,t) \cdot dy \\ \rho(t) = \int_0^1 n(x,t) dx \end{cases}$	Eq. 2.48	[95, 96]

n, numbers of sensitive cells; m, numbers of resistant cells; b_s, birth rate of sensitive cells; d_s, death rate of sensitive cells; u, mutation probability in one cell division; b_s, birth rate of resistant cells; d_s, death rate of resistant cells; P, probability of cell number changing from current generation to the next; S, sensitive cells, R, resistant cells, k_g, k_{g1}, k_{g2}, growth rate constant; d, death rate constant; k_d, shrinkage rate constant as a result of drug treatment; C_D, drug concentration; K_D, drug concentration that produces 50% of maximum treatment effect; dW_1, stochastic cell diffusion in a small time interval (Wiener process); dN_1, stochastic dissemination in a small time interval (Poisson process); σ_1, diffusion rate; q_M, dissemination rate; K, angiogenesis; u_1, u_2, mutation rate; $W(i)$, fitness of type i cell; $Payoff(ij)$, payoff of type i cells when they meet cell type j; p_i, p_j, proportion of cells; r_i, cost of resistance; d_i, cost as a result of treatment; X_i, benefit for resistant cells when interacting with susceptible cells; x, y, resistance levels; $n(x,t)$, cell density with resistance level x at time t; $r(x)$, $r(y)$, cell division rate; $c(x)$, treatment effect; $d(x)$, cell death rate; $G(\rho(t))$, a density dependence term; θ, mutation fraction; $M(y,x)$, probability that cell y mutates to cell x.

Resistance evolution during treatment

The branching process has also been applied to simulate the evolving resistance during treatment. Regarding treatment initiation as the starting point, the dynamics of resistance evolution has been investigated with branching stochastic processes. Starting with a group of drug-sensitive cells, Foo and Michor [80] proposed functions of P_R and E_R during treatment depending on the length of treatment on and break time for continuous and pulsed dosing strategies. Treatment effect was incorporated by setting different birth and death rates for sensitive and resistant cells, if considering partial resistance, at on-treatment and off-treatment periods, respectively. They also estimated P_R, E_R, and variance of resistance cell number during treatment as functions of time considering with or without preexisting resistant cells [81]. Treatment effect in this study was incorporated by making the birth and death rates of both sensitive and (partial) resistant cells affected by drug concentration. The treatment schedule could therefore be optimized by minimizing resistance risk or limiting the size of resistant clones. Corresponding equations were later adopted to simulate the time curve of E_R and P_R, and thereby to identify a relatively best treatment strategy for *EGFR*-mutant NSCLC patients receiving erlotinib [82]. In that study, the birth and death rates of different types of cells were obtained from *in vitro* experiments, and the birth rates were affected by drug concentration [82]. Three cases of mutation rate change because of drug dose were also considered in the study.

Cancer progression under combination therapies has also be investigated with evolution models to predict the outcome of multiple treatment strategies in *EGFR*-mutant lung cancer patients treated with two drugs [83]. Tumor evolution after treatment initiation was modeled as a branching process with at least three types of cells considered: one type of sensitive cell and two types of preexisting resistant cells that are resistant to only one of the two drugs, respectively. The expected numbers of each type of cells were thereby estimated and the sum of which was the total expected cancer cell number (treatment outcome). The treatment effect was described by decreasing the birth rates of cells depending on drug concentration, and drug interaction was also taken into consideration [83].

Besides separating tumor cells as being sensitive and resistant to treatment, one study also separated cells (subclones) according to resistant status and the number of accumulated drivers [84]. In the stochastic branching process of tumor progression, subclones were assumed to have probabilities of raising a driver mutation and a resistant mutation during division. The accumulation of driver mutations resulted in an increase in the fitness of cells, whereas resistance was related to a fitness cost, and the fitness of nonresistant cells decreased because of treatment. By modeling the probability change of each cell type, the expected tumor size and the average frequency of resistant cells were estimated as functions

of time. Subsequently, tumor detection time was calculated and used to compare the effect of prevention and postdiagnostic interventions [84].

Tumor eradication

Considering that resistant mutations may die out as a result of stochastic drift during branching evolution, tumor eradication (treatment success) probability has also been investigated. One study modeled tumor progression as the following three phases: expansion with decreasing division rate until steady state, maintaining steady state, and treatment phase, starting with a single sensitive cell [85]. Treatment was assumed to decrease the division rate and increase the death rate of sensitive cells. A formula of the probability of resistant cells arising but becoming extinct by the end of the treatment in each phase was then proposed, and the overall probability of treatment success was estimated as the product of the three probabilities [85].

Multidrug resistance

The evolution of multidrug resistance has also been elucidated by a stochastic model where drug-sensitive and drug-resistant cells can divide, die (naturally and as a result of treatment), and mutate with certain probabilities [86, 87]. In this model, cells accumulate one mutation that leads to resistance to one drug each time, and all mutations must be accumulated to make a cell resistant to all drugs. The treatment success probability (probability of extinction) as well as the probabilities of resistance when resistant cells generated exclusively before and during treatment were estimated, respectively. Based on the derived equations, the tumor size at which a certain percentage of patients were treated successfully were investigated under various numbers of drugs, mutation rates, and the turnover rates of cancer cells [86, 87]. This model structure and the derived equation of treatment success probability were later utilized to optimize cyclic treatment scheduling [88]. Moreover, taking the contribution of quiescent tumor cells into consideration by incorporating the branching process of both cycling cells and quiescent cells, the effect of quiescent cells on the treatment outcome, such as the resistance probability, of chronic myelogenous leukemia patients has also been investigated [89].

4.2.2 Stochastic differential equation

In addition of the probability models, another stochastic modeling strategy that has been applied to characterize the development of resistance during treatment is by using stochastic differential equations. An example can be found in a study on melanoma cancer patients [90]. Three types of cancer cells, including sensitive, resistant, and metastasis cells, and angiogenetic cells were considered. The dynamics of the number of drug-sensitive cells

is described by Eq. 2.40 (**Table 2.2**). In this differential equation, cell growth, mutation, and death were described deterministically, whereas cell diffusion and dissemination were considered as stochastic processes. Logistic growth function was used to describe the growth of cells, and the mutation from sensitive to resistant cells is described with a first-order process. The death of sensitive cells was caused by drug treatment, and the nonlinear drug exposure-effect relationships was adopted (Eq. 2.40). Wiener process and Poisson process were incorporated to account for stochastic cell diffusion and dissemination, respectively. The effect of angiogenesis was also included. A drug-induced resistance factor, which depends on drug concentrations, was integrated to increase the growth and dissemination rates. The model predictions of the progression-free survival and number of metastasis cells were demonstrated to be, respectively, comparable with the observed progression-free survival and ctDNA level obtained from melanoma patients treated with B-Raf kinase and mitogen-activated protein kinase inhibitors [90].

4.3 Deterministic model

4.3.1 ODEs

Other than stochastic models, deterministic differential equations have also been used to study the evolution toward drug resistance, especially for a population with a large size that often behaves nearly deterministically [13]. The dynamics of sensitive cells and resistant cells can be modeled with ODEs similar to what were introduced in the "Tumor Heterogeneity" section, but the transition from resistant to sensitive cells is often neglected. The model structures that have been identified are shown in **Table 2.2**.

One model of resistance evolution displayed by ODEs is shown as Eq. 2.41, where drug resistance is considered to raise due to point mutations [91]. When considering multiple drug resistance, multiresistant cells were assumed to only be mutated from single-resistant cells. Starting with a certain number of sensitive cells, the resistance amount by the time of treatment initiation and during treatment was estimated under different conditions. The authors demonstrated that the simpler ODE model provided comparable results to previous models that were derived from more complicated stochastic models [91]. Another example can be seen in Eq. 2.42. This model was used to investigate the preferable treatment by controlling the total amount of fully resistant mutants, which can be acquired from sensitive cells and single-resistant cells [88]. In addition, a model with treatment effect being proportional to drug dose has also been used to model evolving tumor resistance (Eq. 2.43) [92]. Multiresistant cells were also considered and were assumed to mutate only from single-resistant cells. Based on this model structure, the survival of patients undergoing

different treatment strategies, such as the strategy of minimizing the total cell population or minimizing the multiresistant population, was investigated [92]. Another model structure of resistance evolution that includes the transition from resistant to sensitive cells (Eq. 2.44) has also been adopted to investigate the optimization of treatment [93].

4.3.2 Game theory

Evolutionary game theory has also been used to investigate the evolution of cancer resistance, especially under combination therapy [94]. It assumes the fitness of one type of cell, which can be understood as the growth rate, changes when the cells interact with different types of other cells. This can be expressed with a payoff matrix, and the final fitness of one type of cell is their expected payoff of this "game" [13]. An example was found from a study where a well-mixed population and a deterministic dynamic of the evolving process were considered [94]. The evolutionary game theory was adopted to investigate and understand the evolving resistance for small cell lung cancer patients under a combination of chemotherapy and tumor suppressor p53 vaccine treatment [94]. Three cell populations, including cells that are sensitive to both treatments and cells that are resistant to one of the treatments but sensitive to the other, were considered to constitute the total tumor population. As presented in **Table 2.2**, the fitness of type i cell can be expressed as a sum of the product of the payoff of type i cell interacting with type j cell and the proportion of type j cell (Eq. 2.45), where a cost of resistance and a cost as a result of treatment was considered [94]. In addition, to account for the influence of cell interaction on cell sensitivity and fitness, an extra benefit for resistant cells when interacting with susceptible cells under treatment was also introduced (Eq. 2.45) [94]. The average fitness was expressed with Eq. 2.46, where pi is the proportion of each type of cells. The dynamics of each cell type under sequencing treatment was described using a replicator equation (Eq. 2.47), and the time curve of the proportion and fitness of each cell type are two main outcomes of the simulations in this study.

4.3.3 Integral-differential equation

An integral-differential equation, where the states of cancer resistance are described in a continuous way ranging from complete sensitivity to complete resistance, has also been used to characterize the evolution of cancer resistance [95, 96]. A model structure shown as Eq. 2.48 has been used to describe the dynamics of cancer cell density with resistance level x at time t [95, 96], where cell division, cell death, treatment effect, and cell mutation were all incorporated (**Table 2.2**). Simulations were performed in these studies to illustrate the evolution of resistant level during treatment, but it has not yet been applied in clinical studies.

5. Model selection

Applying different model structures to characterize tumor dynamics and tumor resistance evolution may achieve different objectives and require different data input and knowledge (**Table 2.3**). The target cancer type and treatment option may also influence the selection of model structure (**Table 2.3**).

As for the tumor dynamics models displayed by ODEs and algebraic equations, most models are applicable to describe tumor size change in patients with various kinds of solid tumors and under different kinds of treatment (monotherapy or combination therapy). However, the models specifically developed for prostate cancer are mainly suitable to describe PSA level change, and the models incorporating angiogenesis biomarkers or immune components are normally considered when patients are treated with antiangiogenesis treatment or immunotherapy, respectively.

Longitudinal tumor size data, such as the SLD of target lesions, MTD, or tumor volumes, or PSA measurements are required to estimate model parameters. A mixed-effect modeling approach has been applied to most model structures that are displayed by ODEs and algebraic equations to account for interindividual variability, whereas the parameters of other structures, such as the two-phase model, were normally estimated for each subject separately. In the former case, each subject in a group is normally required to contribute at least one measurement before treatment and one thereafter. More data points are preferred to enable the better estimate of all parameters. However, the latter method may require each subject to contribute enough data points to enable parameter estimates. In addition, if a study aims at developing a model incorporating biomarkers, longitudinal biomarker observations or previously reported models for treatment-biomarkers interaction are required. If no specific biological process is considered, the selection of model structures can also depend on the model fit to the data as long as the model is physiologically or biologically plausible.

Among the functions of the natural tumor growth (Eqs. 2.1–2.8), which are always part of the tumor dynamics models, the exponential growth model has been the most frequently selected in clinical studies. The logistic growth model was normally satisfactorily applied when the maximum tumor capacity was fixed. The selection of the basic functions could also depend on the model fit to the data. More than one available pretreatment tumor size measurement would be helpful to find the best fit natural growth model and would enable a more accurate estimate of the tumor natural growth rate.

Table 2.3: Data input and knowledge requirement, study type, and objectives (besides characterizing treatment effect in cancer patients) for applying different model structures

Models	Data input and knowledge requirement	Study types	Study objective
Tumor growth models			
Models considering tumor heterogeneity (ODEs)			
Proliferative + Quiescent (Eqs. 2.9–2.10)	• Longitudinal TS measurement • Mechanism of treatment (cell cycle specific or not) • Applicable for different treatments and cancer types • Applicable for monotherapy or combination therapy	• Estimation based study and simulation study • Mixed-effect model possible	• Optimize treatment
Sensitive + Resistant (Eqs. 2.11–2.13)	• Longitudinal TS measurement • Applicable for different treatments and cancer types • Applicable for monotherapy (or combination therapy)	• Estimation based study and simulation study • Mixed-effect model possible	• Identify resistance type (acquired or primary) and mechanism
Model developed by Ideta et al. (Eq. 2.12)	• IAS and CAS • Prostate cancer	• Simulation study	• Describe and predict PSA change under treatment
Model developed by Hirata et al. (Eq. 213)	• Longitudinal PSA measurement • IAS and CAS • Prostate cancer	• Estimation based study • Estimate parameters for each subject	• Describe and predict PSA change under treatment • Optimize treatment • Individualize treatment
Models incorporating biological factors (ODEs)			
Angiogenesis biomarkers (Eq. 214)	• Longitudinal TS measurement • Longitudinal biomarkers measurement or previously reported models for treatment-biomarker interaction • Mechanism of treatment • Applied mainly for antiangiogenesis treatment, monotherapy or combination therapy • Applicable for different cancer types	• Estimation based study • Mixed-effect model possible	• Identify clinically relevant outcome predictors and optimal time to measure the biomarkers

Tumor vascular support (Eqs. 2.15–2.16)	• Longitudinal TS measurement • Mechanism of treatment • Applicable for different treatments and cancer types • Applicable for monotherapy (or combination therapy)	• Estimation based study and simulation study • Mixed-effect model possible	• Optimize treatment
Immune system (Eqs. 2.17–2.18)	• Longitudinal TS / PSA measurement • Immunotherapy • Mechanism of treatment • Applicable for different cancer types	• Estimation based study and simulation study • Estimate parameters for each subject	• Optimize treatment
Immune system (Eqs. 2.19–2.20)	• General cancer • Chemotherapy	• Simulation study	• Optimize treatment
Treatment effect model (ODEs)			
First-order treatment effect (Eq. 2.21)	• Drug dependent • Parameter can be different for different dose group	• Estimation based study and simulation study • Mixed-effect model possible	• Characterize treatment effect
Exposure-dependent treatment effect (Eqs. 2.22–2.25)	• Longitudinal concentration data • Or PK model (newly developed or previously published) for simulating drug exposure, or dose (as a metric of drug exposure) • Applicable for different treatments and cancer types • Applicable for monotherapy or combination therapy • A compartment for damaged cells (Eq. 2.24) applied mainly for chemotherapy and/or radio therapy	• Estimation based study and simulation study • Mixed-effect model possible	• Characterize relationship between tumor size change and treatment exposure • Optimize treatment
Algebraic equation			
Two-phase model (Eqs. 2.26–2.28)	• Longitudinal TS/PSA data • PK information is not necessary • Applicable for different treatments and cancer types • Applicable for monotherapy or combination therapy	• Estimation based study • Estimate parameters for each subject	• Investigate the relationship between tumor growth rate and survival

Table 2.3 continues on next page.

Table 2.3: *Continued*

Models	Data input and knowledge requirement	Study types	Study objective
Model developed by Wang et al. (Eq. 2.29)	• Longitudinal TS data • PK information is not necessary • Applicable for different treatments, monotherapy or combination therapy • Mainly in NSCLC patients	• Estimation based study • Mixed-effect model possible	• Elucidate relationship between metrics of tumor size and survival
Extension of model developed by Wang et al. (Eqs. 2.30–2.31)	• Longitudinal TS data • Mainly in RCC patients treated with pazopanib • Dose-depended treatment effect can be incorporated	• Estimation based study • Mixed-effect model possible	-
Simplified TGI model (Eq. 2.32)	• Longitudinal TS data • PK information is not necessary • Applicable for different treatments and cancer types • Applicable for monotherapy or combination therapy	• Estimation based study • Mixed-effect model possible	• Elucidate relationship between metrics of tumor size and survival
Partial differential equation			
Proliferation-invasion model (Eqs. 2.33–2.38)	• Two pair of T1-Gd and T2 MRI data before treatment • Or one pair of T1-Gd and T2 MRI data before treatment, with available parameters in previous studies • Glioblastoma • Resection, radiotherapy, or without treatment	• Estimation based study and simulation study • Estimate parameters for each subject	• Predict patients' survival and tumor size after treatment • Simulate patients' outcome under different treatment • Personalize treatment • Investigate the application of a novel model
	• DW-MRI data, one before and two after treatment, for tumor cell numbers calculation • Breast cancer patients with neoadjuvant therapy • Consider mass effect	• Estimate parameters for each subject (the growth rate is the net growth rate considering both tumor growth and death)	• Predict tumor burden at the conclusion of treatment.

Tumor resistance evolution models			
Probability model (Eq. 2.39)	• Parameter values (from previous studies or by estimating clinical or pre-clinical data) • If available, longitudinal or static ctDNA measurement can be used to estimate parameters or evaluate simulation results • General cancer and treatment • Single or multidrug resistance	• Simulation study • Apply proposed equations in data obtained in clinical study (mainly in lung cancer, colorectal and leukaemia treated with targeted treatment) • No mixed-effect model applied yet	• Elucidate the resistance evolution of cancer • Propose equations for estimating and investigating $E_{R'}$ $P_{R'}$ total tumor cells, and treatment success rate • Estimate the detection time • Predict treatment outcome and optimize treatment • Demonstrate if resistance exist at the start of treatment
Stochastic differential equation (Eq. 2.40)	• Parameter values (from previous studies or by estimating clinical or pre-clinical data) • Mechanism of treatment • If available, longitudinal ctDNA measurement can be used to evaluate simulation results • Mainly in melanoma patients treated with BRAF and MEK inhibitor	• Simulation study • No mixed-effect model applied yet	• Connect cellular mechanisms underlying cancer drug resistance to patients survival.
ODEs (Eqs. 2.41–2.44)	• General cancer and treatment • Single or multidrug resistance	• Simulation study • No mixed-effect model applied yet	• Predict treatment outcome and optimize treatment • Propose model
Game theory (Eqs. 2.45–2.47)	• Payoff matrix • Combination treatment	• Simulation study • No mixed-effect model applied	• To understand experimental results
Integral-differential equation (Eq. 2.48)	• General cancer and treatment • Single or multidrug resistance	• Simulation study • No mixed-effect model applied	• Describing multidrug resistance • Demonstrating the evolving resistance under treatment

BRAF, B-Raf kinase; CAS, continuous androgen suppression; ctDNA, circulating tumor DNA; DW-MRI, diffusion-weighted MRI; ER, expected number of resistant cells; IAS, intermittent androgen suppression; MEK, mitogen-activated protein kinase; MRI, magnetic resonance images; NSCLC, non-small cell lung cancer; ODEs, ordinary differential equations; PK, pharmacokinetics; PR, probability of resistance; PSA, prostate-specific antigen; RCC, renal cell carcinoma; T1-Gd, gadolinium-enhanced T1 weighted; T2, T2 weighted; TS, tumor size.

The treatment effect can be characterized in a drug-dependent manner or exposure-dependent manner. If a study does not focus on investigating the exposure-effect relationship, using a model with drug-dependent tumor shrinkage will be enough and drug-exposure information is not required. For studies aiming at characterizing the relationship between drug exposure/dose and tumor response and/or optimizing treatment regimens for patients based on simulations, the exposure-dependent (or dose-dependent) treatment effect structure should be applied. To estimate drug exposure, longitudinal concentration data for PK model development or a previously reported PK model are needed. In addition, the previous knowledge of the treatment mechanism may also be required to appropriately characterize the treatment effect, especially when applying models considering biological factors.

The proliferation-invasion model that is displayed by PDE has mainly been applied to investigate glioblastoma or breast cancer based on available MRI measurements. The required parameters can be estimated for each patient separately based on two sets of pretreatment MRI data or one before treatment and one thereafter. Simulations can then be performed to predict patient outcome with the model or with the velocity function of tumor radius expansion (Eq. 2.34). The mixed-effect modeling approach has not been found to be applied in these studies yet.

The model structures of tumor resistance evolution have been mainly applied to perform simulations to understand evolving resistance and optimize the treatment. The equations derived from the branching process can be applied to answer clinical questions. Available longitudinal or static ctDNA measurements can be utilized to determine the parameter values and to evaluate the simulation results. Although no mixed-effect modeling approach has been applied in these studies yet, the model structures displayed by ODEs, which can provide comparable results to stochastic models, are considered to be potentially able to account for interindividual variability.

6. Discussion

Overcoming treatment resistance with a better understanding of cancer evolution and personalizing treatment brings opportunities to treat cancer as a chronic disease and has been increasingly studied in the oncology field. Model-based approaches incorporating tumor growth and resistance evolution may help achieve this goal. By applying mathematical models, prior knowledge derived from clinical trials and routine patients care can be utilized to quantitatively understand drug PK profiles, the drug-response relationship,

and evolving resistance in cancer patients. These profiles can be predicted accordingly for future patients, which could be beneficial for identifying optimized therapeutic regimens. Furthermore, by accounting for interindividual variability with a mixed-effect modeling approach, treatment individualization can also be designed and guided rationally [97].

In the current review, feasible model structures that have been used to describe and predict tumor dynamics and resistance evolution during treatment for patients with solid tumors are discussed. Models concerning tumor evolution in leukemia were included because they provide reference value for solid tumors. Apart from what has been introduced, more extensive models have also been found in the literature search, such as agent-based models and the cellular automata approach. The agent-based models often include components from two or more spatial or temporal scales, ranging from molecular to tissue [7], and the cellular automata approach adopts a discrete dynamical system of time and space [9]. Although tumor growth can be simulated in silico realistically with these approaches, because they require infeasible information input (e.g., cell location, nutrition distribution, and/or oxygen amount) from clinical patients, they were excluded from the current review. Studies applying the proliferation-invasion model, which are expressed with PDE, were not excluded, although tumor cell location is also one of the variables. It is because two main parameters in this model structure, the diffusion coefficient *Dif* and growth rate constant ρ, can be estimated directly based on MRI results obtained from patients, and the velocity of tumor radius expansion can then be estimated and utilized for prediction.

Models displayed by ODEs, algebraic equations, and PDE are commonly reported for the modeling of tumor size change and, in the case of prostate cancer, PSA amount change. Five main basic natural tumor growth model structures were frequently reported. The diversity in model selection can be explained by the difficulties of assessing real long-term natural tumor growth pattern in patients [11]. Although setting the maximum boundaries of tumor growth is more biologically plausible, the models without such limits, especially the exponential growth models, have also been used extensively. The concept of linear growth is also reflected in the studies that applied the proliferation-invasion model, as the expansion of tumor radius has a constant velocity under such a model, and this concept has been used to predict tumor radius [63-65].

For characterizing treatment effect, empirical methods are relatively simple to apply for describing the effect of various kinds of drugs and are therefore more generally applicable. The shrinkage rate of tumor burden caused by treatment can be described to be proportional to drug exposure/dose or by utilizing drug-dependent parameters, although the latter method does not allow differentiation among different dosing regimens. In addition,

when the dynamics of biomarkers are available and are incorporated in the tumor dynamics models, the treatment effect on the production of biomarkers can be integrated according to drug mechanism [31, 39]. Furthermore, the regrowth of a tumor during treatment can be considered in several ways. Studies applying algebraic equations generally characterize the decline and regrowth of a tumor by a single equation. For studies that used ODEs, tumor regrowth was mainly characterized by separating the tumor in two parts consisting of drug-sensitive cells and drug-resistant cells or by adding the $e^{-\lambda \cdot t}$ term.

The resistance evolution of cancer has been mainly characterized by stochastic models within which the branching process is reported most frequently. However, in studies applying the branching process, the focus was mainly on the expected outcome of tumor evolution, such as the P_R and E_R. Therefore, relatively simpler deterministic models are considered to be good alternative choices. It has already been demonstrated that ODE models can provide comparable results to those that are derived from stochastic models [91]. Given that the goal is to characterize evolving tumor resistance based on clinical data, applying deterministic models might be more suitable given clinical available data generally represents the apparent response of each patient.

Among the studies included in this review, the detailed data of resistance evolution have not yet been incorporated in tumor size-based modeling of anticancer treatment response. However, genetic biomarkers that represent tumor heterogeneity and resistance evolution become increasingly available as a result of novel technologies. For example, in a clinical setting, a feasible genetic biomarker that is also correlated with tumor burden has been identified as ctDNA [98]. Three of the included studies have already utilized the available ctDNA data to support the estimation of parameters in the tumor evolution model or to evaluate the model simulation results [77, 79, 90]. It has also been demonstrated that the mutation in ctDNA, which represents treatment resistance, is detectable before disease progression [99], suggesting the predictive value of ctDNA to the development of drug resistance. By applying longitudinal monitoring of ctDNA, an adaptive treatment for individual patients may be achieved by selecting drugs that target emerging actionable mutations [98]. Therefore, it is feasible to obtain the information of evolving cancer resistance and, to increase the chance to overcome treatment resistance, it would be helpful if such information could be incorporated in future model-based studies.

Based on what was learned from previous reported studies, as is introduced in this review, model structures displayed by ODEs are considered to be feasible for the characterization of both tumor size change and resistance evolution in cancer patients. A mathematical model can be developed based on the input data of tumor size, mutation load of ctDNA,

and treatment information over time. The emergence and dynamics of mutations in ctDNA can provide insight of the occurrence, growth, decay, and mutation for different tumor subclones. External data sets, if available, can be used to further evaluate the developed model structure. Subsequently, the effect of sequential treatment regimens with different dose levels or starting times of therapies can be explored with simulation and thereby to facilitate the identification of an optimal regimen. Moreover, because the parameter values can be estimated for each individual and the variability of which can be partially explained by patient characteristics, the treatment personalization can also be rationally guided based on the modeling and simulation results. These will be the ultimate output of the model-based study.

However, challenges remain beyond what is already stated. First, in terms of data collection, previous knowledge of the mutations that represent resistant subclones is required. Second, if sequencing data of the subclones (ctDNA) over time are available, efforts need to be made to handle the vast amount of genetic data in a quantitative manner in relation to tumor size dynamics. Third, the optimal method on how to predict a newly acquired mutation that has not yet occurred in the data needs to be further explored. Finally, because in-depth knowledge is required from multiple aspects of tumor and clone dynamics as well as complex modeling and simulation, a multidisciplinary collaboration is essential to enable the achievement of the ultimate goal of optimizing and personalizing anticancer treatment.

In conclusion, based on a systematic search of studies from the literature, mathematical models that have been used to describe and predict tumor size change, drug effect, and resistance evolution based on clinically available data were introduced in this review. The results may facilitate the model-based anticancer treatment response analysis that accounts for both tumor growth inhibition and resistance evolution, although important challenges still need to be overcome. An ultimate model structure handling all of these aspects would be of great benefit for optimizing and personalizing anticancer treatment.

References

1. Sun X, Hu B. Mathematical modeling and computational prediction of cancer drug resistance. Brief Bioinform. 2018;19(6):1382-99. doi:10.1093/bib/bbx065.
2. Beksac AT, Paulucci DJ, Blum KA, Yadav SS, Sfakianos JP, Badani KK. Heterogeneity in renal cell carcinoma. Urol Oncol. 2017;35(8):507-15. doi:10.1016/j.urolonc.2017.05.006.
3. Buil-Bruna N, Lopez-Picazo JM, Martin-Algarra S, Troconiz IF. Bringing Model-Based Prediction to Oncology Clinical Practice: A Review of Pharmacometrics Principles and Applications. Oncologist. 2016;21(2):220-32. doi:10.1634/theoncologist.2015-0322.
4. Kimko H, Pinheiro J. Model-based clinical drug development in the past, present and future: a commentary. Br J Clin Pharmacol. 2015;79(1):108-16. doi:10.1111/bcp.12341.
5. van Hasselt JG, van der Graaf PH. Towards integrative systems pharmacology models in oncology drug development. Drug Discov Today Technol. 2015;15:1-8. doi:10.1016/j.ddtec.2015.06.004.
6. Barbolosi D, Ciccolini J, Lacarelle B, Barlesi F, Andre N. Computational oncology--mathematical modelling of drug regimens for precision medicine. Nat Rev Clin Oncol. 2016;13(4):242-54. doi:10.1038/nrclinonc.2015.204.
7. Wang Z, Butner JD, Kerketta R, Cristini V, Deisboeck TS. Simulating cancer growth with multiscale agent-based modeling. Semin Cancer Biol. 2015;30:70-8. doi:10.1016/j.semcancer.2014.04.001.
8. Meghdadi N, Soltani M, Niroomand-Oscuii H, Ghalichi F. Image based modeling of tumor growth. Australas Phys Eng Sci Med. 2016;39(3):601-13. doi:10.1007/s13246-016-0475-5.
9. Masoudi-Nejad A, Bidkhori G, Hosseini Ashtiani S, Najafi A, Bozorgmehr JH, Wang E. Cancer systems biology and modeling: microscopic scale and multiscale approaches. Semin Cancer Biol. 2015;30:60-9. doi:10.1016/j.semcancer.2014.03.003.
10. Ribba B, Holford NH, Magni P, Troconiz I, Gueorguieva I, Girard P, et al. A review of mixed-effects models of tumor growth and effects of anticancer drug treatment used in population analysis. CPT Pharmacometrics Syst Pharmacol. 2014;3:e113. doi:10.1038/psp.2014.12.
11. Bender BC, Schindler E, Friberg LE. Population pharmacokinetic-pharmacodynamic modelling in oncology: a tool for predicting clinical response. Br J Clin Pharmacol. 2015;79(1):56-71. doi:10.1111/bcp.12258.
12. Kim C, Gao R, Sei E, Brandt R, Hartman J, Hatschek T, et al. Chemoresistance Evolution in Triple-Negative Breast Cancer Delineated by Single-Cell Sequencing. Cell. 2018;173(4):879-93 e13. doi:10.1016/j.cell.2018.03.041.
13. Beerenwinkel N, Schwarz RF, Gerstung M, Markowetz F. Cancer evolution: mathematical models and computational inference. Syst Biol. 2015;64(1):e1-25. doi:10.1093/sysbio/syu081.
14. Zhao B, Hemann MT, Lauffenburger DA. Modeling Tumor Clonal Evolution for Drug Combinations Design. Trends Cancer. 2016;2(3):144-58. doi:10.1016/j.trecan.2016.02.001.
15. Chisholm RH, Lorenzi T, Clairambault J. Cell population heterogeneity and evolution towards drug resistance in cancer: Biological and mathematical assessment, theoretical treatment optimisation. Biochim Biophys Acta. 2016;1860(11 Pt B):2627-45. doi:10.1016/j.bbagen.2016.06.009.
16. Attolini CS, Michor F. Evolutionary theory of cancer. Ann N Y Acad Sci. 2009;1168:23-51. doi:10.1111/j.1749-6632.2009.04880.x.
17. Foo J, Michor F. Evolution of acquired resistance to anti-cancer therapy. J Theor Biol. 2014;355:10-20. doi:10.1016/j.jtbi.2014.02.025.
18. Stein A, Wang W, Carter AA, Chiparus O, Hollaender N, Kim H, et al. Dynamic tumor modeling of the dose–response relationship for everolimus in metastatic renal cell carcinoma using data from the phase 3 RECORD-1 trial. BMC Cancer. 2012;12:311.

19. Cameron DA, Gregory WM, Bowman A, Anderson ED, Levack P, Forouhi P, et al. Identification of long-term survivors in primary breast cancer by dynamic modelling of tumour response. Br J Cancer. 2000;83(1):98-103. doi:10.1054/bjoc.2000.1216.
20. Claret L, Girard P, Hoff PM, Van Cutsem E, Zuideveld KP, Jorga K, et al. Model-based prediction of phase III overall survival in colorectal cancer on the basis of phase II tumor dynamics. J Clin Oncol. 2009;27(25):4103-8. doi:10.1200/jco.2008.21.0807.
21. De Buck SS, Jakab A, Boehm M, Bootle D, Juric D, Quadt C, et al. Population pharmacokinetics and pharmacodynamics of BYL719, a phosphoinositide 3-kinase antagonist, in adult patients with advanced solid malignancies. Br J Clin Pharmacol. 2014;78(3):543-55. doi:10.1111/bcp.12378.
22. Panetta JC, Schaiquevich P, Santana VM, Stewart CF. Using pharmacokinetic and pharmacodynamic modeling and simulation to evaluate importance of schedule in topotecan therapy for pediatric neuroblastoma. Clin Cancer Res. 2008;14(1):318-25. doi:10.1158/1078-0432.ccr-07-1243.
23. Ideta AM, Tanaka G, Takeuchi T, Aihara K. A Mathematical Model of Intermittent Androgen Suppression for Prostate Cancer. Journal of Nonlinear Science. 2008;18(6):593-614. doi:10.1007/s00332-008-9031-0.
24. Ollier E, Mazzocco P, Ricard D, Kaloshi G, Idbaih A, Alentorn A, et al. Analysis of temozolomide resistance in low-grade gliomas using a mechanistic mathematical model. Fundam Clin Pharmacol. 2017;31(3):347-58. doi:10.1111/fcp.12259.
25. Ribba B, Kaloshi G, Peyre M, Ricard D, Calvez V, Tod M, et al. A tumor growth inhibition model for low-grade glioma treated with chemotherapy or radiotherapy. Clin Cancer Res. 2012;18(18):5071-80. doi:10.1158/1078-0432.CCR-12-0084.
26. Atuegwu NC, Arlinghaus LR, Li X, Welch EB, Chakravarthy BA, Gore JC, et al. Integration of diffusion-weighted MRI data and a simple mathematical model to predict breast tumor cellularity during neoadjuvant chemotherapy. Magn Reson Med. 2011;66(6):1689-96. doi:10.1002/mrm.23203.
27. Belfatto A, Riboldi M, Ciardo D, Cecconi A, Lazzari R, Jereczek-Fossa BA, et al. Adaptive Mathematical Model of Tumor Response to Radiotherapy Based on CBCT Data. IEEE journal of biomedical and health informatics. 2016;20(3):802-9. doi:10.1109/jbhi.2015.2453437.
28. Yu RX, Holmgren E. Endpoints for agents that slow tumor growth. Contemp Clin Trials. 2007;28(1):18-24. doi:10.1016/j.cct.2006.05.011.
29. Bethge A, Schumacher U, Wedemann G. Simulation of metastatic progression using a computer model including chemotherapy and radiation therapy. J Biomed Inform. 2015;57:74-87. doi:10.1016/j.jbi.2015.07.011.
30. Simeoni M, Magni P, Cammia C, De Nicolao G, Croci V, Pesenti E, et al. Predictive pharmacokinetic-pharmacodynamic modeling of tumor growth kinetics in xenograft models after administration of anticancer agents. Cancer Res. 2004;64(3):1094-101.
31. Ouerdani A, Goutagny S, Kalamarides M, Troconiz IF, Ribba B. Mechanism-based modeling of the clinical effects of bevacizumab and everolimus on vestibular schwannomas of patients with neurofibromatosis type 2. Cancer Chemother Pharmacol. 2016;77(6):1263-73. doi:10.1007/s00280-016-3046-2.
32. Stura I, Venturino E, Guiot C. A two-clones tumor model: Spontaneous growth and response to treatment. Math Biosci. 2016;271:19-28. doi:10.1016/j.mbs.2015.10.014.
33. Gardner SN. Modeling multi-drug chemotherapy: tailoring treatment to individuals. J Theor Biol. 2002;214(2):181-207. doi:10.1006/jtbi.2001.2459.
34. Morken JD, Packer A, Everett RA, Nagy JD, Kuang Y. Mechanisms of resistance to intermittent androgen deprivation in patients with prostate cancer identified by a novel computational method. Cancer Res. 2014;74(14):3673-83. doi:10.1158/0008-5472.can-13-3162.

35. Yang J, Zhao TJ, Yuan CQ, Xie JH, Hao FF. A nonlinear competitive model of the prostate tumor growth under intermittent androgen suppression. J Theor Biol. 2016;404:66-72. doi:10.1016/j.jtbi.2016.05.033.
36. Hirata Y, Bruchovsky N, Aihara K. Development of a mathematical model that predicts the outcome of hormone therapy for prostate cancer. J Theor Biol. 2010;264(2):517-27. doi:10.1016/j.jtbi.2010.02.027.
37. Tanaka G, Hirata Y, Goldenberg SL, Bruchovsky N, Aihara K. Mathematical modelling of prostate cancer growth and its application to hormone therapy. Philosophical transactions Series A, Mathematical, physical, and engineering sciences. 2010;368(1930):5029-44. doi:10.1098/rsta.2010.0221.
38. Hirata Y, Azuma S, Aihara K. Model predictive control for optimally scheduling intermittent androgen suppression of prostate cancer. Methods. 2014;67(3):278-81. doi:10.1016/j.ymeth.2014.03.018.
39. Hansson EK, Amantea MA, Westwood P, Milligan PA, Houk BE, French J, et al. PKPD Modeling of VEGF, sVEGFR-2, sVEGFR-3, and sKIT as Predictors of Tumor Dynamics and Overall Survival Following Sunitinib Treatment in GIST. CPT Pharmacometrics Syst Pharmacol. 2013;2:e84. doi:10.1038/psp.2013.61.
40. Ouerdani A, Struemper H, Suttle AB, Ouellet D, Ribba B. Preclinical Modeling of Tumor Growth and Angiogenesis Inhibition to Describe Pazopanib Clinical Effects in Renal Cell Carcinoma. CPT Pharmacometrics Syst Pharmacol. 2015;4(11):660-8. doi:10.1002/psp4.12001.
41. Mellal L, Folio D, Belharet K, Ferreira A. Modeling of Optimal Targeted Therapies Using Drug-Loaded Magnetic Nanoparticles for Liver Cancer. IEEE Trans Nanobioscience. 2016;15(3):265-74. doi:10.1109/tnb.2016.2535380.
42. Ledzewicz U, Marriott J, Maurer H, Schattler H. Realizable protocols for optimal administration of drugs in mathematical models for anti-angiogenic treatment. Math Med Biol. 2010;27(2):157-79. doi:10.1093/imammb/dqp012.
43. Bunimovich-Mendrazitsky S, Halachmi S, Kronik N. Improving Bacillus Calmette-Guerin (BCG) immunotherapy for bladder cancer by adding interleukin 2 (IL-2): a mathematical model. Math Med Biol. 2016;33(2):159-88. doi:10.1093/imammb/dqv007.
44. Kronik N, Kogan Y, Elishmereni M, Halevi-Tobias K, Vuk-Pavlovic S, Agur Z. Predicting outcomes of prostate cancer immunotherapy by personalized mathematical models. PLoS One. 2010;5(12):e15482. doi:10.1371/journal.pone.0015482.
45. De Pillis LG, Radunskaya A. The dynamics of an optimally controlled tumor model: A case study. Math Comput Model. 2003;37(11):1221-44. doi:Pii S0895-7177(03)00133-X. doi 10.1016/S0895-7177(03)00133-X.
46. Lobato FS, Machado VS, Steffen V, Jr. Determination of an optimal control strategy for drug administration in tumor treatment using multi-objective optimization differential evolution. Comput Methods Programs Biomed. 2016;131:51-61. doi:10.1016/j.cmpb.2016.04.004.
47. de Pillis LG, Gu W, Fister KR, Head T, Maples K, Murugan A, et al. Chemotherapy for tumors: an analysis of the dynamics and a study of quadratic and linear optimal controls. Math Biosci. 2007;209(1):292-315. doi:10.1016/j.mbs.2006.05.003.
48. Majid O, Gupta A, Reyderman L, Olivo M, Hussein Z. Population pharmacometric analyses of eribulin in patients with locally advanced or metastatic breast cancer previously treated with anthracyclines and taxanes. J Clin Pharmacol. 2014;54(10):1134-43. doi:10.1002/jcph.315.
49. Zecchin C, Gueorguieva I, Enas NH, Friberg LE. Models for change in tumour size, appearance of new lesions and survival probability in patients with advanced epithelial ovarian cancer. Br J Clin Pharmacol. 2016;82(3):717-27. doi:10.1111/bcp.12994.

50. Stein WD, Figg WD, Dahut W, Stein AD, Hoshen MB, Price D, et al. Tumor growth rates derived from data for patients in a clinical trial correlate strongly with patient survival: a novel strategy for evaluation of clinical trial data. Oncologist. 2008;13(10):1046-54. doi:10.1634/theoncologist.2008-0075.
51. Stein WD, Gulley JL, Schlom J, Madan RA, Dahut W, Figg WD, et al. Tumor regression and growth rates determined in five intramural NCI prostate cancer trials: the growth rate constant as an indicator of therapeutic efficacy. Clin Cancer Res. 2011;17(4):907-17. doi:10.1158/1078-0432.ccr-10-1762.
52. Wang Y, Sung C, Dartois C, Ramchandani R, Booth BP, Rock E, et al. Elucidation of relationship between tumor size and survival in non-small-cell lung cancer patients can aid early decision making in clinical drug development. Clin Pharmacol Ther. 2009;86(2):167-74. doi:10.1038/clpt.2009.64.
53. Bonate PL, Suttle AB. Modeling tumor growth kinetics after treatment with pazopanib or placebo in patients with renal cell carcinoma. Cancer Chemother Pharmacol. 2013;72(1):231-40. doi:10.1007/s00280-013-2191-0.
54. Claret L, Gupta M, Han K, Joshi A, Sarapa N, He J, et al. Evaluation of tumor-size response metrics to predict overall survival in Western and Chinese patients with first-line metastatic colorectal cancer. J Clin Oncol. 2013;31(17):2110-4. doi:10.1200/JCO.2012.45.0973.
55. Stein WD, Yang J, Bates SE, Fojo T. Bevacizumab reduces the growth rate constants of renal carcinomas: a novel algorithm suggests early discontinuation of bevacizumab resulted in a lack of survival advantage. Oncologist. 2008;13(10):1055-62. doi:10.1634/theoncologist.2008-0016.
56. Li CH, Bies RR, Wang Y, Sharma MR, Karovic S, Werk L, et al. Comparative Effects of CT Imaging Measurement on RECIST End Points and Tumor Growth Kinetics Modeling. Clin Transl Sci. 2016;9(1):43-50. doi:10.1111/cts.12384.
57. Claret L, Mercier F, Houk BE, Milligan PA, Bruno R. Modeling and simulations relating overall survival to tumor growth inhibition in renal cell carcinoma patients. Cancer Chemother Pharmacol. 2015;76(3):567-73. doi:10.1007/s00280-015-2820-x.
58. Claret L, Bruno R, Lu JF, Sun YN, Hsu CP. Exploratory modeling and simulation to support development of motesanib in Asian patients with non-small cell lung cancer based on MONET1 study results. Clin Pharmacol Ther. 2014;95(4):446-51. doi:10.1038/clpt.2014.11.
59. Han K, Claret L, Sandler A, Das A, Jin J, Bruno R. Modeling and simulation of maintenance treatment in first-line non-small cell lung cancer with external validation. BMC Cancer. 2016;16:473. doi:10.1186/s12885-016-2455-2.
60. Han K, Claret L, Piao Y, Hegde P, Joshi A, Powell JR, et al. Simulations to Predict Clinical Trial Outcome of Bevacizumab Plus Chemotherapy vs. Chemotherapy Alone in Patients With First-Line Gastric Cancer and Elevated Plasma VEGF-A. CPT Pharmacometrics Syst Pharmacol. 2016;5(7):352-8. doi:10.1002/psp4.12064.
61. Swanson KR, Rostomily RC, Alvord EC, Jr. A mathematical modelling tool for predicting survival of individual patients following resection of glioblastoma: a proof of principle. Br J Cancer. 2008;98(1):113-9. doi:10.1038/sj.bjc.6604125.
62. Mandonnet E, Pallud J, Clatz O, Taillandier L, Konukoglu E, Duffau H, et al. Computational modeling of the WHO grade II glioma dynamics: principles and applications to management paradigm. Neurosurg Rev. 2008;31(3):263-9. doi:10.1007/s10143-008-0128-6.
63. Wang CH, Rockhill JK, Mrugala M, Peacock DL, Lai A, Jusenius K, et al. Prognostic significance of growth kinetics in newly diagnosed glioblastomas revealed by combining serial imaging with a novel biomathematical model. Cancer Res. 2009;69(23):9133-40. doi:10.1158/0008-5472.can-08-3863.

64. Rockne R, Rockhill JK, Mrugala M, Spence AM, Kalet I, Hendrickson K, et al. Predicting the efficacy of radiotherapy in individual glioblastoma patients in vivo: a mathematical modeling approach. Phys Med Biol. 2010;55(12):3271-85. doi:10.1088/0031-9155/55/12/001.
65. Szeto MD, Chakraborty G, Hadley J, Rockne R, Muzi M, Alvord EC, Jr., et al. Quantitative metrics of net proliferation and invasion link biological aggressiveness assessed by MRI with hypoxia assessed by FMISO-PET in newly diagnosed glioblastomas. Cancer Res. 2009;69(10):4502-9. doi:10.1158/0008-5472.can-08-3884.
66. Le M, Delingette H, Kalpathy-Cramer J, Gerstner ER, Batchelor T, Unkelbach J, et al. Personalized Radiotherapy Planning Based on a Computational Tumor Growth Model. IEEE Trans Med Imaging. 2017;36(3):815-25. doi:10.1109/tmi.2016.2626443.
67. Murray JD. Glioblastoma brain tumours: estimating the time from brain tumour initiation and resolution of a patient survival anomaly after similar treatment protocols. J Biol Dyn. 2012;6 Suppl 2:118-27. doi:10.1080/17513758.2012.678392.
68. Yankeelov TE, Atuegwu N, Hormuth D, Weis JA, Barnes SL, Miga MI, et al. Clinically relevant modeling of tumor growth and treatment response. Sci Transl Med. 2013;5(187):187ps9. doi:10.1126/scitranslmed.3005686.
69. Weis JA, Miga MI, Arlinghaus LR, Li X, Abramson V, Chakravarthy AB, et al. Predicting the Response of Breast Cancer to Neoadjuvant Therapy Using a Mechanically Coupled Reaction-Diffusion Model. Cancer Res. 2015;75(22):4697-707. doi:10.1158/0008-5472.can-14-2945.
70. Weis JA, Miga MI, Arlinghaus LR, Li X, Chakravarthy AB, Abramson V, et al. A mechanically coupled reaction-diffusion model for predicting the response of breast tumors to neoadjuvant chemotherapy. Phys Med Biol. 2013;58(17):5851-66. doi:10.1088/0031-9155/58/17/5851.
71. Harpold HL, Alvord EC, Jr., Swanson KR. The evolution of mathematical modeling of glioma proliferation and invasion. J Neuropathol Exp Neurol. 2007;66(1):1-9. doi:10.1097/nen.0b013e31802d9000.
72. Sakkalis V, Roniotis A, Farmaki C, Karatzanis I, Marias K. Evaluation framework for the multilevel macroscopic models of solid tumor growth in the glioma case. Conf Proc IEEE Eng Med Biol Soc. 2010;2010:6809-12. doi:10.1109/iembs.2010.5625961.
73. Patel V, Hathout L. Image-driven modeling of the proliferation and necrosis of glioblastoma multiforme. Theor Biol Med Model. 2017;14(1):10. doi:10.1186/s12976-017-0056-7.
74. Hathout L, Ellingson B, Pope W. Modeling the efficacy of the extent of surgical resection in the setting of radiation therapy for glioblastoma. Cancer Sci. 2016;107(8):1110-6. doi:10.1111/cas.12979.
75. Cross W, Graham TA, Wright NA. New paradigms in clonal evolution: punctuated equilibrium in cancer. J Pathol. 2016;240(2):126-36. doi:10.1002/path.4757.
76. Iwasa Y, Nowak MA, Michor F. Evolution of resistance during clonal expansion. Genetics. 2006;172(4):2557-66. doi:10.1534/genetics.105.049791.
77. Diaz LA, Jr., Williams RT, Wu J, Kinde I, Hecht JR, Berlin J, et al. The molecular evolution of acquired resistance to targeted EGFR blockade in colorectal cancers. Nature. 2012;486(7404):537-40. doi:10.1038/nature11219.
78. Komarova NL, Burger JA, Wodarz D. Evolution of ibrutinib resistance in chronic lymphocytic leukemia (CLL). Proc Natl Acad Sci U S A. 2014;111(38):13906-11. doi:10.1073/pnas.1409362111.
79. Bozic I, Nowak MA. Timing and heterogeneity of mutations associated with drug resistance in metastatic cancers. Proc Natl Acad Sci U S A. 2014;111(45):15964-8. doi:10.1073/pnas.1412075111.
80. Foo J, Michor F. Evolution of resistance to targeted anti-cancer therapies during continuous and pulsed administration strategies. PLoS Comput Biol. 2009;5(11):e1000557. doi:10.1371/journal.pcbi.1000557.

81. Foo J, Michor F. Evolution of resistance to anti-cancer therapy during general dosing schedules. J Theor Biol. 2010;263(2):179-88. doi:10.1016/j.jtbi.2009.11.022.
82. Liu LL, Li F, Pao W, Michor F. Dose-Dependent Mutation Rates Determine Optimum Erlotinib Dosing Strategies for EGFR Mutant Non-Small Cell Lung Cancer Patients. PLoS One. 2015;10(11):e0141665. doi:10.1371/journal.pone.0141665.
83. Chakrabarti S, Michor F. Pharmacokinetics and Drug Interactions Determine Optimum Combination Strategies in Computational Models of Cancer Evolution. Cancer Res. 2017;77(14):3908-21. doi:10.1158/0008-5472.can-16-2871.
84. Akhmetzhanov AR, Hochberg ME. Dynamics of preventive vs post-diagnostic cancer control using low-impact measures. eLife. 2015;4:e06266. doi:10.7554/eLife.06266.
85. Bozic I, Allen B, Nowak MA. Dynamics of targeted cancer therapy. Trends Mol Med. 2012;18(6):311-6. doi:10.1016/j.molmed.2012.04.006.
86. Komarova N. Stochastic modeling of drug resistance in cancer. J Theor Biol. 2006;239(3):351-66. doi:10.1016/j.jtbi.2005.08.003.
87. Komarova NL, Wodarz D. Drug resistance in cancer: principles of emergence and prevention. Proc Natl Acad Sci U S A. 2005;102(27):9714-9. doi:10.1073/pnas.0501870102.
88. Katouli AA, Komarova NL. The worst drug rule revisited: mathematical modeling of cyclic cancer treatments. Bull Math Biol. 2011;73(3):549-84. doi:10.1007/s11538-010-9539-y.
89. Komarova NL, Wodarz D. Effect of cellular quiescence on the success of targeted CML therapy. PLoS One. 2007;2(10):e990. doi:10.1371/journal.pone.0000990.
90. Sun X, Bao J, Shao Y. Mathematical Modeling of Therapy-induced Cancer Drug Resistance: Connecting Cancer Mechanisms to Population Survival Rates. Sci Rep. 2016;6:22498. doi:10.1038/srep22498.
91. Tomasetti C, Levy D. An elementary approach to modeling drug resistance in cancer. Mathematical biosciences and engineering : MBE. 2010;7(4):905-18. doi:10.3934/mbe.2010.7.905.
92. Beckman RA, Schemmann GS, Yeang CH. Impact of genetic dynamics and single-cell heterogeneity on development of nonstandard personalized medicine strategies for cancer. Proc Natl Acad Sci U S A. 2012;109(36):14586-91. doi:10.1073/pnas.1203559109.
93. Ledzewicz U, Wang S, Schattler H, Andre N, Heng MA, Pasquier E. On drug resistance and metronomic chemotherapy: A mathematical modeling and optimal control approach. Mathematical biosciences and engineering : MBE. 2017;14(1):217-35. doi:10.3934/mbe.2017014.
94. Basanta D, Gatenby RA, Anderson AR. Exploiting evolution to treat drug resistance: combination therapy and the double bind. Mol Pharm. 2012;9(4):914-21. doi:10.1021/mp200458e.
95. Greene J, Lavi O, Gottesman MM, Levy D. The impact of cell density and mutations in a model of multidrug resistance in solid tumors. Bull Math Biol. 2014;76(3):627-53. doi:10.1007/s11538-014-9936-8.
96. Lavi O, Greene JM, Levy D, Gottesman MM. The role of cell density and intratumoral heterogeneity in multidrug resistance. Cancer Res. 2013;73(24):7168-75. doi:10.1158/0008-5472.can-13-1768.
97. Agur Z, Elishmereni M, Kheifetz Y. Personalizing oncology treatments by predicting drug efficacy, side-effects, and improved therapy: mathematics, statistics, and their integration. Wiley Interdiscip Rev Syst Biol Med. 2014;6(3):239-53. doi:10.1002/wsbm.1263.
98. Wan JCM, Massie C, Garcia-Corbacho J, Mouliere F, Brenton JD, Caldas C, et al. Liquid biopsies come of age: towards implementation of circulating tumour DNA. Nat Rev Cancer. 2017;17(4):223-38. doi:10.1038/nrc.2017.7.
99. Xiong L, Cui S, Ding J, Sun Y, Zhang L, Zhao Y, et al. Dynamics of EGFR mutations in plasma recapitulates the clinical response to EGFR-TKIs in NSCLC patients. Oncotarget. 2017;8(38):63846-56. doi:10.18632/oncotarget.19139.

Supplementary Material S2.1

Literature searching method

As for tumor dynamic modelling, a search term: ("Models, Theoretical" [Majr:NoExp] OR "Computer Simulation"[Mesh] OR "Models, Biological*" [Majr:NoExp]) AND ("mathematical" [title/abstract] OR "computational"[title/abstract] OR "model-based"[title/abstract] OR "model based" [title/abstract] OR "pharmacometric*"[title/abstract] OR model framework[title/abstract] OR modelling framework[title/abstract] OR modeling framework[title/abstract] OR PK/PD model* [title/abstract] OR PK-PD model* [title/abstract]) AND (pharmacody* [title/abstract] OR tumor growth[title/abstract] OR tumour growth[title/abstract] OR tumor dynamic[title/abstract] OR tumour dynamic[title/abstract] OR tumor dynamics[title/abstract] OR tumour dynamics[title/abstract] OR tumor-growth[title/abstract] OR tumour-growth[title/abstract] OR "change in tumor size"[title/abstract] OR "change in tumour size"[title/abstract] OR "tumor growth inhibition"[title/abstract] OR "tumour growth inhibition"[title/abstract]) AND ("Neoplasms"[Majr:NoExp] OR "cancer"[title/abstract] OR "tumor*"[title/abstract] OR "tumour*"[title/abstract] OR malignan*[title/abstract] OR oncolog*[title/abstract]) AND "Humans"[Mesh] NOT "Animals"[Mesh:NoExp] NOT "Cells"[Mesh] AND English[Language] AND (Pharmacology OR oncology) was used to retrieve records from PubMed database. Papers published until the start of March 2018 were scanned based on their abstract and method part. Papers that met the following criteria were included: 1) published after 2000; 2) studies where longitudinal tumor size data obtained from patients with solid tumors was described with mathematical models; 3) studies where longitudinal PSA data from prostate cancer patients was characterized with mathematical models; 4) studies where tumor size data from patients were obtained to estimate model parameters; 5) reviews that summarized equations of different tumor growth modelling structures; 6) simulation studies where the models are potentially applicable in clinical settings, i.e. well mixed cancer cell population were considered.

Exclusion criteria include: 1) studies published before 2000; 2) studies for which the full text was not available; 3) animal studies; 4) computer aided molecular studies; 5) studies with no equation reported; 6) studies characterizing disease progression; 7) studies that focus on MRI/PET/CT utility, optimization, or kinetics; 8) studies characterizing safety and toxicity profiles; 9) studies characterizing the dynamic of biomarkers or markers related to drug activity; 10) studies where the target cancer types are not solid tumor; 11) studies that modelled cell cycle kinetics or signaling pathway; 12) computational methodology studies; 13) studies characterizing tumor evolution; 14) introductory journal article; 15)

reviews discussing the application of mathematical models and/or have no equations reported; 16) other studies that are not focus on tumor growth analysis; 17) simulation studies where the models are potentially not feasible in clinical settings, including studies considered nutrition distribution, cellular automata, multiple scales, chemical potential, and in silico illustration of tumor growth .

As for tumor resistance evolution modelling, a search term: ("Models, Theoretical" [Mesh] OR "Computer Simulation"[Mesh] OR "Models, Biological*" [Mesh]) AND ("mathematical" [title/abstract] OR "computational"[title/abstract] OR "model-based"[title/abstract] OR "model based"[title/abstract] OR "pharmacometric*"[title/abstract] OR model framework[title/abstract] OR modelling framework[title/abstract] OR modeling framework[title/abstract]) AND ("Neoplasms"[Majr:NoExp] OR "cancer"[title/abstract] OR "tumor*"[title/abstract] OR "tumour*"[title/abstract] OR malignan*[title/abstract] OR oncolog*[title/abstract]) AND "Humans"[Mesh] NOT "Cells"[Mesh] AND English[Language] AND ("Drug Resistance, Neoplasm"[mesh] OR "Biological Evolution"[Majr:NoExp] OR "Clonal Evolution"[Mesh]) AND ("Resistance"[title/abstract] OR " heterogeneit* "[title/abstract] OR "evolution"[title/abstract] OR "clone"[title/abstract] OR microenvironment[title/abstract]) was used to retrieve records from PubMed database. Papers published until the start of March 2018 were scanned based on their abstract and method part. Papers that met the following criteria were included: 1) published after 2000; 2) model-based studies on the evolution of tumor resistance and tumor progression; 3) reviews that summarized equations of different model structure.

Exclusion criteria include: 1) studies published before 2000; 2) articles that overlap with what we obtained from tumor growth modelling; 3) studies for which the full text was not available; 4) computational molecular studies; 5) network studies; 6) studies concerning P-glycoprotein and resistance protein; 7) studies focus on cell cycle kinetics or signaling pathway; 8) introductory journal article; 9) studies characterizing tumor growth; 10) studies with no equation reported; 11) reviews discussing the application of models and/or have no equations reported; 12) other studies that are not focus on tumor evolution.

Studies concerning tumor dynamics and tumor resistance evolution that were retrieved by the other search term were also scanned and included according to their own corresponding inclusion and exclusion criteria respectively. Included articles' references which introduced corresponding original models or demonstrated application examples, which were not found in the included papers, of certain model structures were included as well.

The flow diagram of scanning literature is shown in **Figure S2.1**.

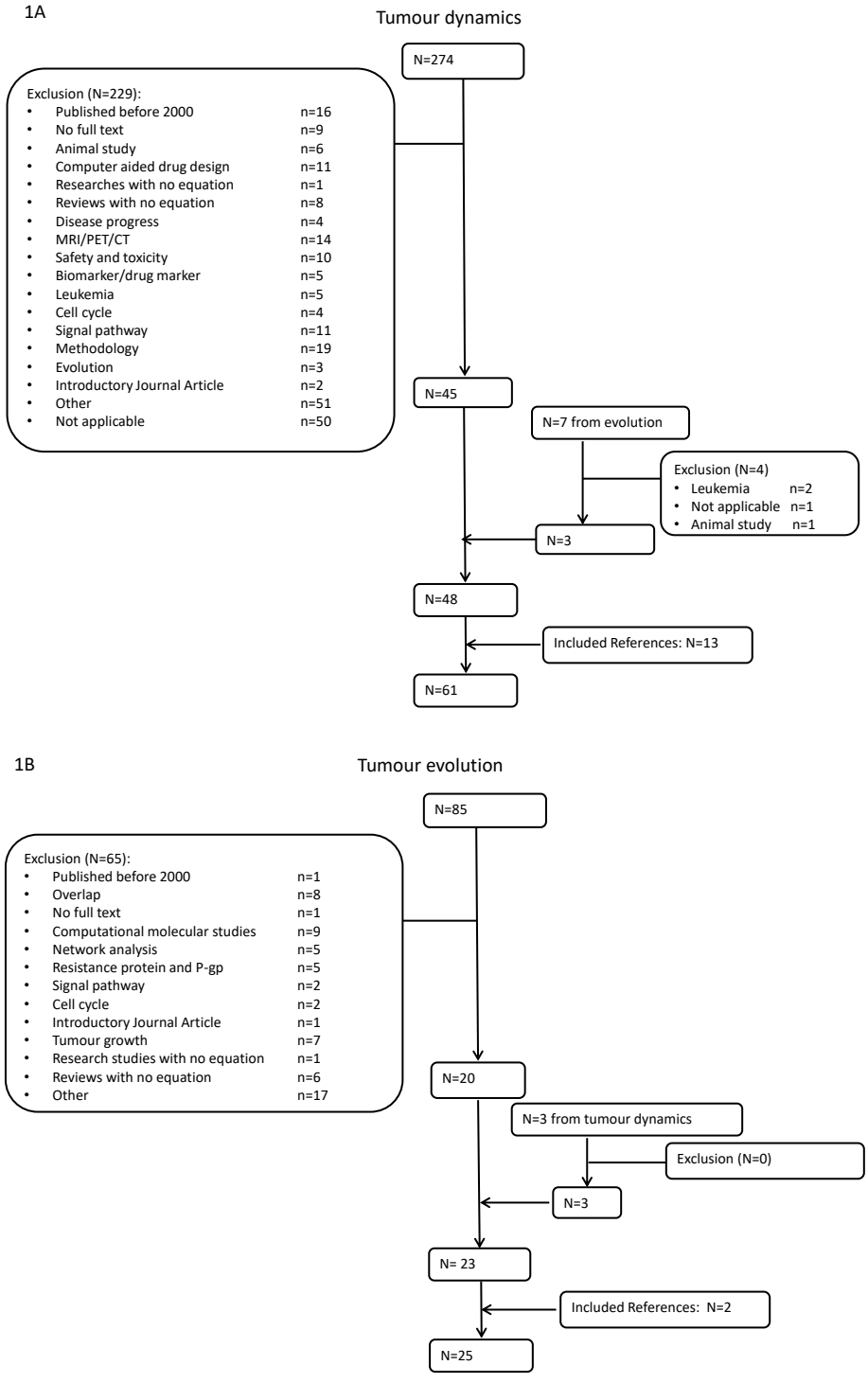

Figure S2.1: Diagram of literature scanning for (A) tumor dynamics and (B) tumor resistance evolution.

Software

Software that was applied in studies concerning tumor dynamics (TD) and tumor evolution (TE) to perform parameter estimation and data simulation is summarized in **Table S2.1**. As can be seen in the table, NONMEM and Matlab are two most frequently used software that performing model-based analysis concerning tumor dynamics. Studies applying non-linear mixed-effect models (NLMEM) mostly utilized NONMEM software to estimate parameter values, while Matlab was popular when performing simulation with partial differential equations. Three other commonly used software packages for tumor dynamics modelling are Monolix, Phoenix NLME, and Sigmaplot. For studies performing tumor evolution analysis, only a few of them reported the software, namely Matlab and R.

Table S2.1: Software that was applied in studies concerning tumor dynamics (TD) and tumor evolution (TE) to perform parameter estimation and data simulation

Application	Name	Algorithm
TD	NONMEM (ICON Development Solutions)	First-order conditional estimation with interaction (FOCE-I) algorithm
		First-order conditional estimation (FOCE) algorithm
		Laplacian algorithm
		Stochastic approximation of expectation minimization (SAEM) algorithm
	Matlab	Ordinary differential equation solver
		pdepe
		ODE45 subroutine
		A custom genetic algorithm
	Monolix	SAEM algorithm
	Phoenix NLME	FOCE algorithm
	Sigmaplot (Systat Software Inc)	Not mentioned
	SPLUS	Not mentioned
	C programme	Not mentioned
TE	Matlab	Not mentioned
	R; coded with C++	Not mentioned